



Characterization of Joint Roughness Heterogeneity and Its Application in Representative Sample Investigations

Shi-Gui Du^{1,2} · Hang Lin³ · Rui Yong^{1,2} · Guang-Jian Liu^{1,2}

Received: 13 November 2019 / Accepted: 23 February 2022 / Published online: 19 March 2022
© The Author(s) 2022

Abstract

Rock joint surface roughness is usually characterized by heterogeneity, but the determination of a required number of samples for achieving a reasonable heterogeneity assessment remains a challenge. In this paper, a novel method, the global search method, was proposed to investigate the heterogeneity of rock joint roughness. In this method, the roughness heterogeneity was characterized based on a statistical analysis of the roughness of all samples extracted from different locations of a given rock joint. Analyses of the effective sample number were conducted, which showed that sampling bias was caused by an inadequate number of samples. To overcome this drawback, a large natural slate joint sample (1000 mm × 1000 mm in size) was digitized in a laboratory using a high-accuracy laser scanner. The roughness heterogeneities of both two-dimensional (2D) profiles and three-dimensional (3D) surface topographies were systematically investigated. The results show that the expected value obtained from conventional methods failed to accurately represent the overall roughness. The relative errors between the population parameter and the expected value varied not only from sample to sample but also with the scale. The roughness heterogeneity characteristics of joint samples of various sizes can be obtained using the global search method. This new method could facilitate the determination of the most representative samples and their positions.

Highlights

- We propose the global search method to investigate the heterogeneity of roughness.
- Analyses of the effective sample number are conducted to prove the sampling bias.
- We investigate roughness heterogeneity by 2D profiles and 3D surface topographies.
- The method is applied to determining the most representative samples.

Keywords Heterogeneity · Rock joint · Sampling method · Scale effect

Abbreviations

JRC Joint roughness coefficient
JCS Joint wall compressive strength

2D Two-dimensional
3D Three-dimensional
SP Starting point
SI Sampling interval
EP End point

✉ Rui Yong
yongrui@nbu.edu.cn

¹ School of Civil and Environmental Engineering,
Ningbo University, Ningbo, Zhejiang 315211,
People's Republic of China

² Key Laboratory of Rock Mechanics and Geohazards
of Zhejiang Province, Shaoxing University, Shaoxing,
Zhejiang 312000, People's Republic of China

³ School of Resources and Safety Engineering,
Central South University, Changsha, Hunan 410083,
People's Republic of China

List of symbols

A_{\max} Maximum profile amplitude
 A Local asperity amplitude
 A_0 Maximum potential contact area ratio
 A_{θ}^* Contact area ratio that is the normalized area of triangles with an apparent dip greater than a threshold value θ^*
 C A fitting parameter that describes the shape of the cumulative distribution
 d Absolute error

D	Fractal dimension
h	The number of all the combinations of any two individual samples in \mathbb{R}
H	Joint roughness heterogeneity
J_i^*	Roughness parameter in the measured roughness population
l	Length of the joint sample
L	Length of the large joint profile
L_t	The true profile length
n	Number of selected individual samples
n_0	Effective sample number
N	Total number of individual samples
r	The margin of error
r'	Relative error
r_i	Normalizing roughness parameter
R_p	Roughness profile index or profile sinuosity
SI	Sampling interval
S	The standard deviation of a population
\hat{S}	Standard deviation of some individual samples
t	The bilateral quantile of the standard normal distribution under a confidence level of $1-\alpha$
u	Undulation factor
Z_2'	First-derivative root-mean-square
Z_2	Modified root-mean-square
φ_b	Basic friction angle
λ	Percentage of the abandoned part of the joint profile
$1-\alpha$	Confidence level
θ	Population parameter
η_i	Representativeness coefficient
θ^*	Inclination of the area along the shear direction
θ_{\max}^*	Maximum apparent dip angle along the shear direction
$\hat{\theta}$	Expected value
$V(\hat{\theta})$	Sampling variance
\mathbb{R}	Joint roughness population of samples taken from different positions

1 Introduction

Joint roughness affects the mechanical and hydraulic behavior of fractured rock masses (Bae et al. 2011; Chen et al. 2021; Lê et al. 2018; Yong et al. 2018d; Zhang et al. 2017; Zhao et al. 2018). During the last 4 decades, considerable efforts have been devoted to the quantitative description of the surface roughness of rock joints (Barton 1978; Fardin 2007; Grasselli et al. 2002; Kulatilake and Um 1999; Liu et al. 2017; Maerz et al. 1990; Morelli 2014; Tse and Cruden 1979; Zheng and Qi 2016; Ban et al. 2021). However, given the variability and limited accessibility of natural features, achieving an exact characterization of in situ fractures is generally difficult (Vogler et al. 2017). Natural

discontinuities often show spatial variations of roughness (Alameda-Hernández et al. 2014; Wu et al. 2020). The uncertainty in the joint roughness measurements greatly affects the estimation of the rock joint shear strength and further influences the evaluation of the rock mass stability.

Based on rock joint roughness investigations in the field, Du (1998) summarized the following three characteristics of joint roughness: (1) heterogeneity, (2) anisotropy, and (3) nonuniformity. Heterogeneity indicates that the joint roughness measurement varies with position, even when measured on the same joint surface and along the same measurement direction, because the roughness varies considerably along different cross-sections of a joint surface. Anisotropy indicates that the joint roughness behaves differently in different directions, even when measured on the same joint surface, which is attributed to the formation process of rock joints. Nonuniformity indicates that the joint roughness is dependent on the type of rock, mineral grain size, and the weathering conditions. Joint roughness estimations are generally performed on a set of joint profiles measured parallel to the direction of the shear displacement for a given rock joint, and the average value is commonly used to represent the roughness of the entire joint surface (Diaz et al. 2017; Du 1999; Liu et al. 2017; Lopez et al. 2003; Tang et al. 2015; Xia et al. 2014; Zhang et al. 2016). The International Society for Rock Mechanics (ISRM) advised obtaining surface roughness from rock joint samples located at different positions and of varied length scales (Ulusay and Hudson 2006). These studies have already considered the influence of heterogeneity on joint roughness estimations and are helpful for obtaining representative evaluation results. However, the areal extent of the exposed joint surface in situ is generally limited, so researchers often have to evaluate the joint roughness based on insufficient samples. Sampling bias is an important issue in statistics and likely leads to incorrect predictions (Spiegel and Stephens 2017). Thus, researchers need to know how many individuals they must survey to draw conclusions about the population. In this study, the population refers to all samples extracted from different locations of a given rock joint, and an individual refers to one of the potential samples. In previous studies, investigators have not paid enough attention to the influence of the sample number, and the problem of estimating the joint roughness based on an inadequate number of samples remains unsolved.

Many investigations have been conducted on the scale effect of shear strength through laboratory and in situ tests (Bandis et al. 1981; Fardin et al. 2001; Hencher and Richards 2014; Tatone and Grasselli 2012; Ye et al. 2016). It was found that the selection of testing samples affects the observation of scale effects, and sampling bias may lead to incorrect conclusions about the scale effect (Barton 1990). For example, representative joint samples of different sizes are

needed to accurately describe the scale-dependent behavior of shear strength. In addition, the average value of the samples subdividing a large joint is used to represent the shear strength of each size, and the relationship between the average value and sample size is used to reveal the scale effect on the shear strength of rock joints (Bahaaddini et al. 2014; Bandis et al. 1981; Morelli 2014). However, the number of joint samples used in previous studies sometimes appears to be insufficient for statistically investigating the scale effect on shear strength (Yong et al. 2018b), which may lead to the inability to estimate the representative characteristics of the scale effect. In practice, the evaluation of structurally controlled slope instability requires careful investigations of the shear behavior of the potential sliding plane (Huang et al. 2019; Tang et al. 2017; Yang et al. 2019a, 2019b). Thus, the representative roughness of the potential sliding plane should be estimated. Systematically characterizing the heterogeneity of joint roughness is expected to provide insights into the exploration of representative samples. Unfortunately, methods for handling the heterogeneity of the surface roughness of rock joints are still lacking.

To address these concerns, the global search method was introduced to characterize the heterogeneity based on a statistical analysis of the roughness of all samples extracted from different locations of a given rock joint. The roughness heterogeneities of both two-dimensional (2D) profiles and three-dimensional (3D) surface topographies were quantitatively evaluated, and then this proposed method was applied for searching representative samples.

2 Heterogeneity of Joint Roughness and Its Investigation in the Field

The accuracy of heterogeneity investigations depends on several factors, such as the accessibility of the plane of interest, the areal extent of the exposed plane, and human error. However, generally, very limited portions of potential sliding planes are exposed in the field. Thus, it is practical to study the heterogeneity of the rock joint roughness based on the exposed part of the potential sliding plane. In rock engineering practice, three situations of exposed potential sliding planes are commonly encountered in field surveys (labeled situations A, B, and C in Fig. 1).

Situation A reflects the case in which a very limited area of a rock joint surface is exposed, and the direction of the long edge of the exposed area is approximately the same as the sliding direction (Fig. 1a and Fig. 2). In this situation, measuring large joint profiles is feasible, and the scale effect on the joint roughness can be investigated. However, it is difficult to obtain many profiles parallel to the sliding direction. To study the heterogeneity, Du (1994, 1999) suggested that the joint roughness should be determined based on the segments (S1, S2, S3, ...) obtained by evenly dividing the measured large joint profile (Fig. 2). The roughness of the entire joint profile is represented on the basis of the average joint roughness coefficient (JRC) of each segment.

Situation B also describes the case where a small area of the rock joint surface is exposed, but the direction of the short edge of the exposed area is the same as the sliding direction (Figs. 1b and 2). In this situation, sufficient profiles (P1, P2, P3, ...) can easily be obtained along the sliding direction (Fig. 2). However, it is not feasible to measure the large joint profiles along the sliding direction in this case. The obtained profiles are too short to investigate the scale

Fig. 1 Three typical situations of the exposed sliding plane commonly encountered in the field. **a** Situation A, **b** situation B, **c** situation C

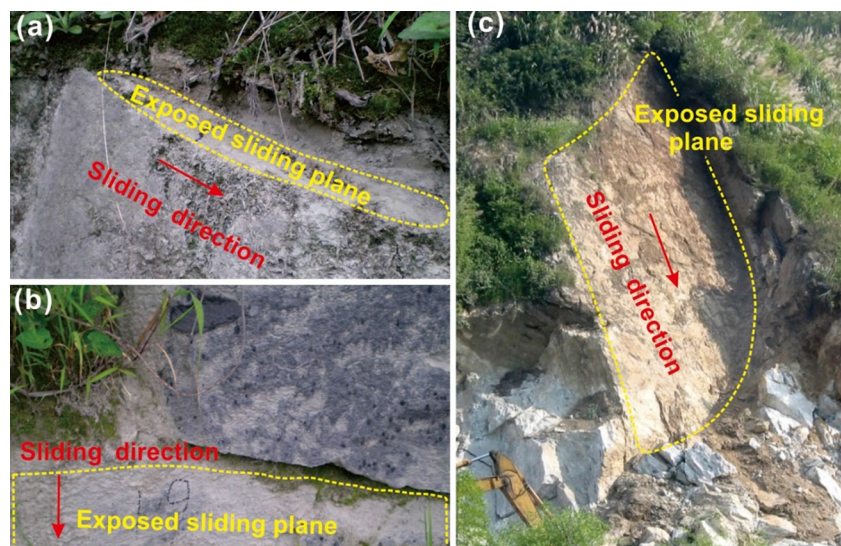
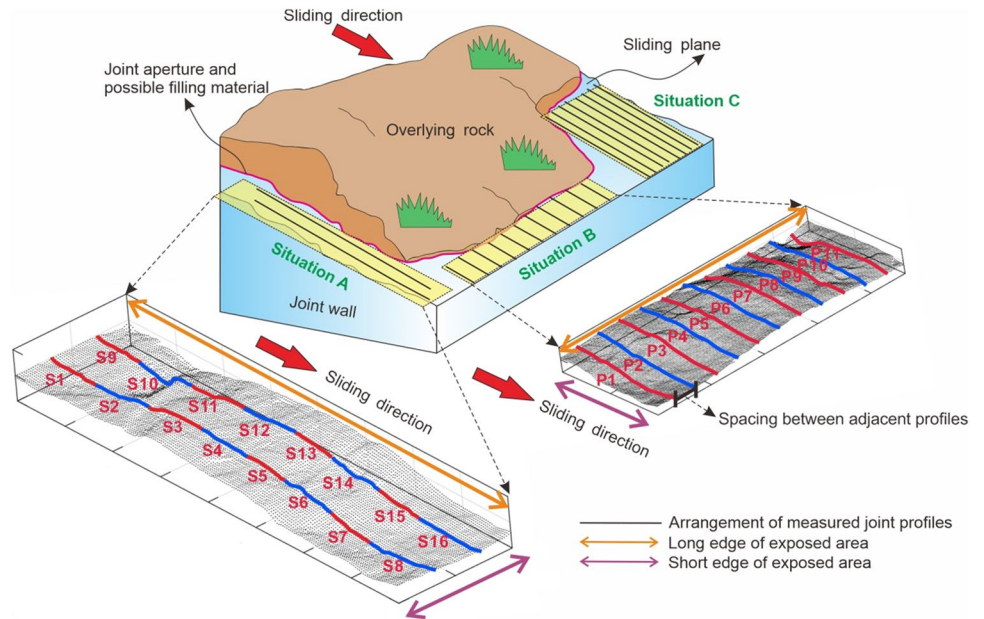


Fig. 2 Arrangement of the measured joint profiles under different situations



effect on the joint roughness. In this situation, the heterogeneity reflects the roughness diversity of small joint profiles (P1, P2, P3, ...) measured at different positions parallel to the sliding direction, and the average roughness of these profiles was used to represent the overall roughness of the studied rock joint.

Situation C describes the case in which a relatively large area of the rock joint surface is exposed (Figs. 1c and 2). In contrast with situations A and B, situation C offers a better condition for measurement, and therefore, obtaining sufficient joint profiles is easier to achieve. In this situation, the

heterogeneity of the joint roughness is relatively comprehensively revealed. As shown in Fig. 2, a number of closely spaced long profiles can be easily measured, and the variation of joint roughness along the parallel profiles can be obtained to characterize the roughness heterogeneity.

For samples with small sizes, acquiring many cross-sections along the potential shear direction is difficult to achieve in situation A. This study focuses on the sampling problem in situation A, and a new method for acquiring sufficient samples is offered to exploit detailed roughness information about the heterogeneity of the joint roughness.

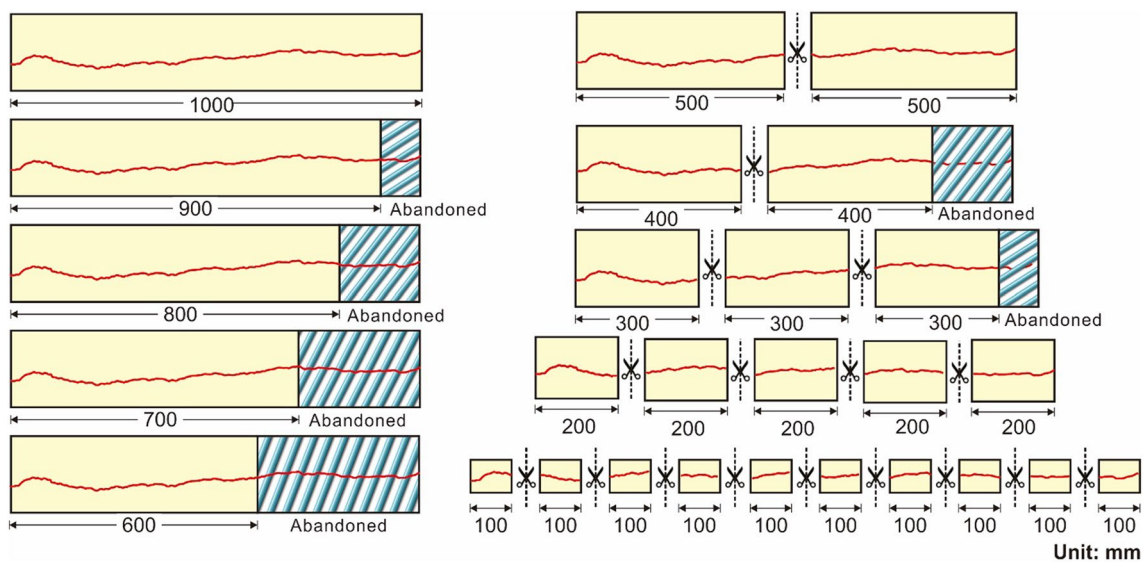


Fig. 3 Samples of different sizes taken from the original surface by the partition sampling method

3 Global Search Method for Investigating the Heterogeneity of Joint Roughness

The conventional sampling methods include the following three categories: (1) the equal-partition sampling method, (2) the simple random sampling method, and (3) the progressive magnifying sampling method. Their definitions and limitations are summarized as follows:

The equal-partition sampling method refers to the sampling process by which smaller sized samples are obtained using equal partitioning of a larger sample. As shown in Fig. 3, we can obtain 100 mm, 200 mm, and 500 mm samples using equal partitioning of the entire joint profile. The obtained samples of each sample size cover the entire length of the original joint. However, for the samples with lengths of 300 mm, 400 mm, 600 mm, 700 mm, 800 mm

and 900 mm, the end parts of the entire joint must be abandoned, because the whole length of the joint profile cannot be equally divided by these sample sizes. For example, when a 600-mm-long sample is taken from the entire joint profile, the length of the abandoned part reaches 40% of the overall length of the original joint. Thus, the roughness of the obtained 600 mm sample can only represent the roughness characteristics of the entire joint in the first 600 mm of length. The roughness characteristics of the abandoned part are neglected. Thus, sampling bias occurs as a result of the samples obtained unable to represent all the samples at different locations on the joint.

The simple random sampling method refers to the sampling process in which samples of different sizes are arbitrarily taken from the original surface. Compared with the equal-partition sampling method, the locations of different-sized samples obtained using the simple random sampling



Fig. 4 Samples of different sizes taken from the original surface by the simple random sampling method

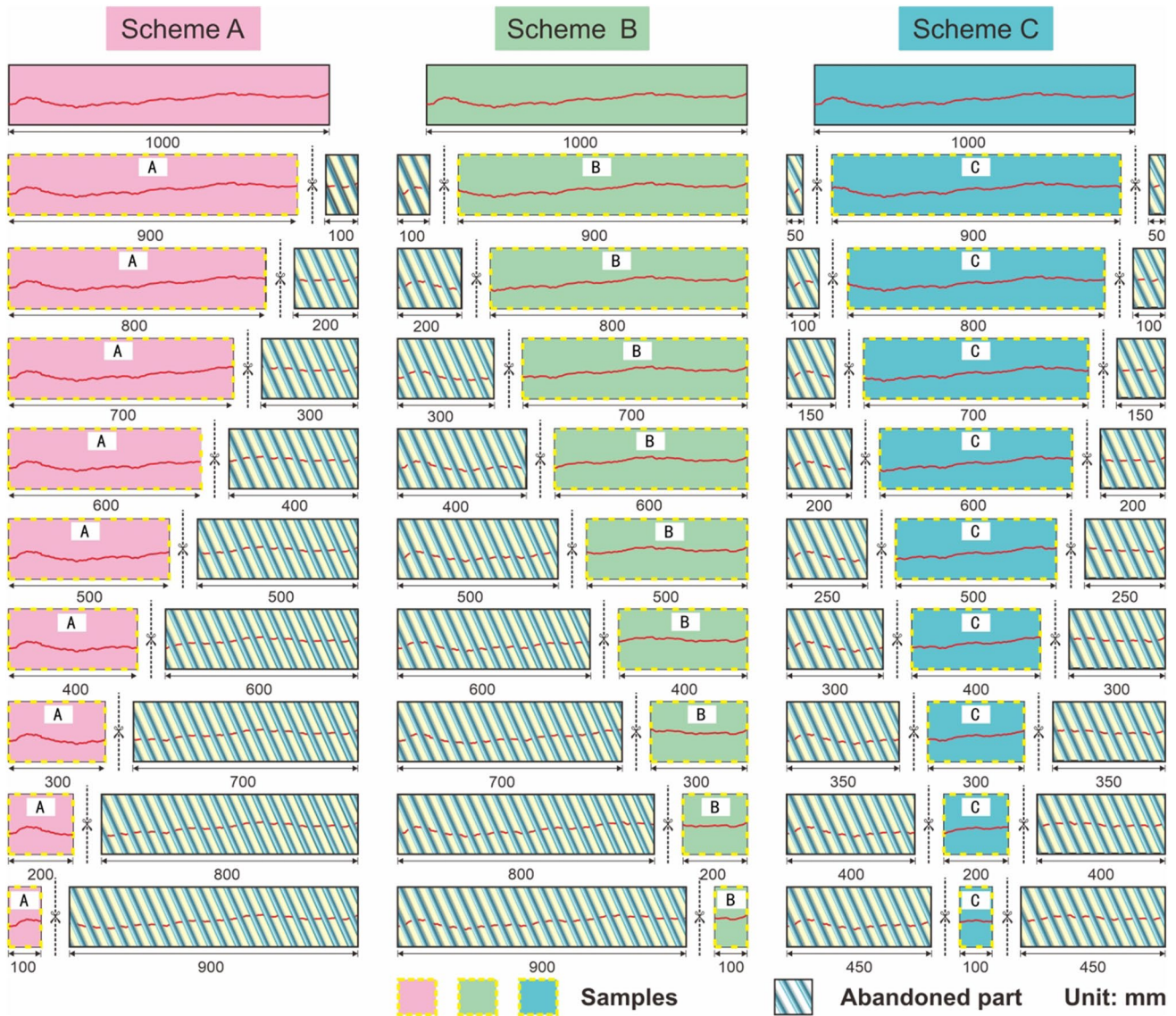


Fig. 5 Samples of different sizes taken from the original surface by the processive magnifying sampling method

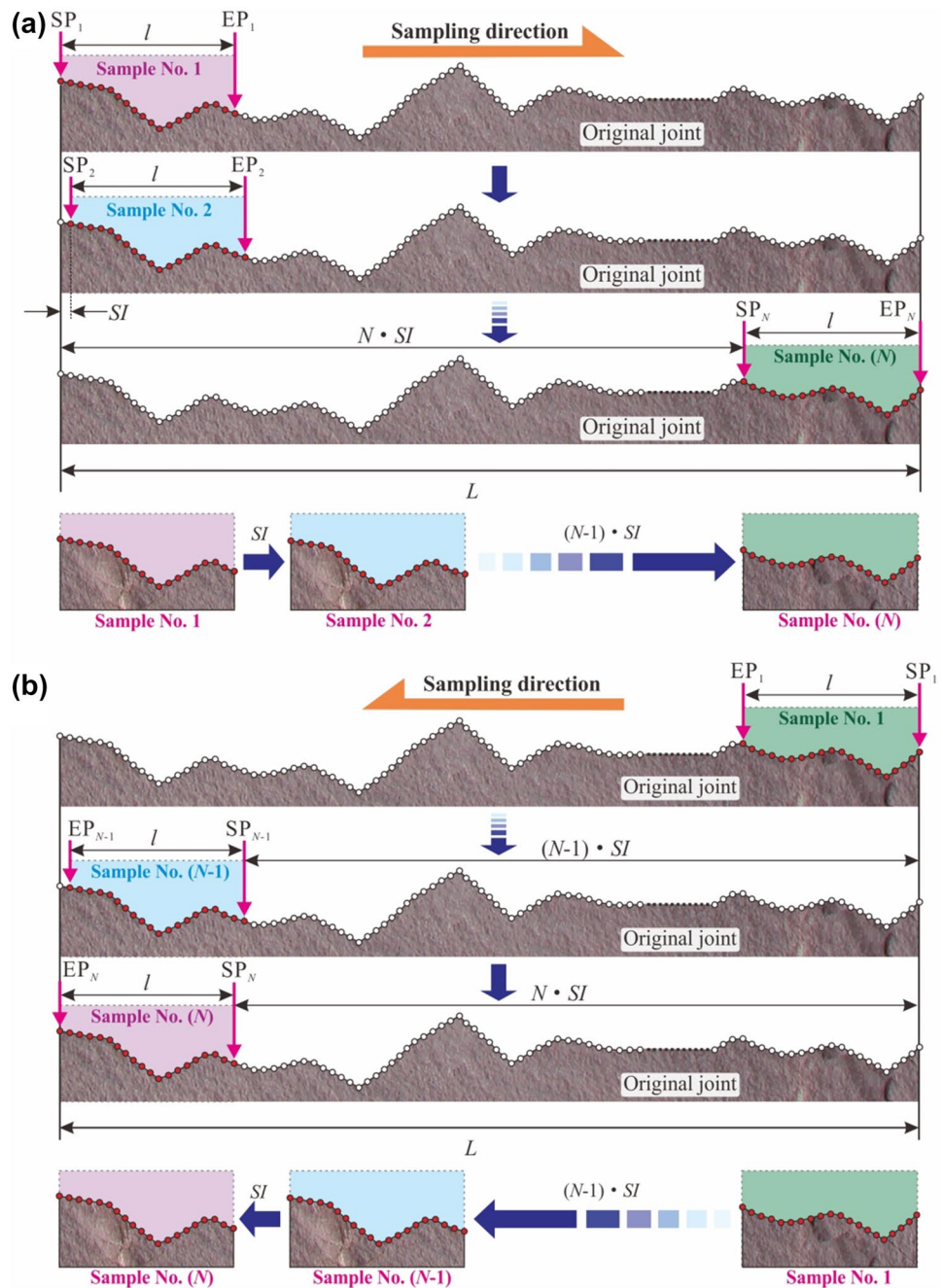
method are random and irregular, and only one sample is selected for each sample size. Figure 4 shows three examples of the sampling schemes obtained based on the simple random sampling method. The locations of the samples obtained in schemes A, B, and C are significantly different, and the morphology of the samples of the same size are also different. The representativeness of samples primarily depends on the personal judgment and choice of researchers, so the sampling results are generally difficult to be reproduced.

The processive magnifying sampling method refers to the sampling process in which smaller sized samples are obtained by an edge cutout from a side section or by cutting a sample from the middle section. Three sampling results are obtained based on the processive magnifying sampling

method, as shown in Fig. 5, where scheme A acquires samples starting from the left edge, scheme B acquires samples starting from the right edge, and scheme C acquires samples starting from the middle. All smaller sized samples are part of larger samples. Compared to the simple random sampling method, the processive magnifying sampling method has explicit sampling rules by which sampling results can be reproduced by different researchers. However, the representativeness of the obtained samples is unclear.

For the simple random sampling method, the sampling results primarily depend on personal judgment, the representativeness of different-sized samples are not quantitatively evaluated. For the equal-partition sampling method and the processive magnifying sampling method, the heterogeneity of joint roughness is not fully considered, and

Fig. 6 Schematic diagram of the global search method



the representativeness of joint samples is not quantitatively evaluated. To solve the sampling problem, the global search method was introduced to characterize the heterogeneity. The roughness profile of a natural rock joint surface is continuous, while the digitized roughness profile data obtained by measurement devices are available only at a certain interval of horizontal spacing (Kulatilake and Um 1999; Li and Zhang 2015; Yong et al. 2018d). Here, the sampling interval

of a digitized profile was labeled SI , the length of the original profile was labeled L , and the lengths of the samples located within the profile ($l \leq L$) were labeled l (Fig. 6). The process of evaluating the overall roughness based on the roughness of different samples is, in essence, a process of representing the characteristics of a population by evaluating the selected individual samples. As shown in Fig. 6, there were many joint samples (Sample No.1 to Sample No. (N))

taken from different positions. The total number of individual samples N depends on SI , which can be given as follows:

$$N = \frac{L-l}{SI} + 1. \tag{1}$$

The joint roughness population of samples taken from different positions can be expressed as follows:

$$\mathbb{R} = \{R_1, R_2, \dots, R_N\}. \tag{2}$$

For instance, for an original profile with a length of $L = 1000$ mm, the number N of the samples with a length of $l = 100$ mm can be calculated by Eq. (1). Based on the above sampling process, we can obtain $N = 1801$ samples under a sampling interval of $SI = 0.5$ mm. However, as shown in Fig. 3, only ten individual samples can be obtained using the partition sampling method.

As shown in Fig. 6, the samples were extracted from different positions on the original profile by moving an SI distance each time. All the individual samples in the population can be obtained based on this sampling process. The change in the starting point (SP) and the end point (EP) makes each sample independent from the other samples. Sufficient samples can be obtained using the global search method without abandoning any side sections of the original profile. Furthermore, the same sampling result can be obtained from the forward and backward directions of the rock joint profile (Fig. 6a, b).

Generally, heterogeneity refers to a phenomenon in which individual trials have results that are different from each other. Here, the characterization of the heterogeneity is based on the analysis of the roughness differences of all individual samples. Heterogeneity indicates that rock joint roughness measurements vary with position, which is inversely proportional to the similarity between individual samples. The smaller similarity between any two joint samples taken from different positions indicates higher heterogeneity, and vice versa.

Let $T = (t_1, t_2, \dots, t_m)$ and $R = (r_1, r_2, \dots, r_m)$ be two m -dimensional vectors. Then, the similarity measures between the two vectors T and R are calculated by the Jacard similarity measure (Ye 2014) as follows:

$$J(T, R) = \frac{T \cdot R}{\|T\|_2^2 + \|R\|_2^2 - T \cdot R} = \frac{\sum_{i=1}^m t_i r_i}{\sum_{i=1}^m t_i^2 + \sum_{i=1}^m r_i^2 - \sum_{i=1}^m t_i r_i}, \tag{3}$$

where $T \cdot R = \sum_{i=1}^m t_i r_i$ is the inner product of the vectors T and R , and $\|T\|_2 = \sqrt{\sum_{i=1}^m t_i^2}$ and $\|R\|_2 = \sqrt{\sum_{i=1}^m r_i^2}$ are the Euclidean norms of T and R , respectively.

Regarding the anisotropy of joint surface roughness, many researchers have suggested that the roughness parameters should be calculated in different directions for full characterization of the 3D surface roughness (Grasselli et al. 2002, Tatone and Grasselli et al. 2012). Let $R_i = (r_{i1}, r_{i2}, \dots, r_{im})$ and $R_j = (r_{j1}, r_{j2}, \dots, r_{jm})$ ($R_i, R_j \in \mathbb{R}, i \neq j$) be two m -dimensional vectors of joint roughness. Here, m is the number of orientations. R_i and R_j represent the roughness individual samples in different orientations of any two samples.

Take the directional roughness $\theta_{\max}^*/[C + 1]_{3D}$ of a sample as an example. The roughness was calculated in directions between 0° and 360° in 5° increments. Thus, the number of the orientations m is 73. Then, the joint roughness vectors can be expressed by $R_i = (r_{i1}, r_{i2}, \dots, r_{i73})$. Here, r_{i1} is the obtained roughness in direction of 0° , r_{i2} is the obtained roughness in direction of 5° , ..., and r_{i73} is the obtained roughness in direction of 360° .

The joint roughness heterogeneity can be quantified as follows:

$$H = \frac{1}{h} \sum_{R_i, R_j \in \mathbb{R}} \frac{\|R_i\|_2^2 + \|R_j\|_2^2 - R_i \cdot R_j}{R_i \cdot R_j} = \frac{1}{h} \sum_{R_i, R_j \in \mathbb{R}} \frac{\sum_{k=1}^m r_{ik}^2 + \sum_{k=1}^m r_{jk}^2 - \sum_{k=1}^m r_{ik} r_{jk}}{\sum_{i=1}^m r_{ik} r_{jk}}, \tag{4}$$

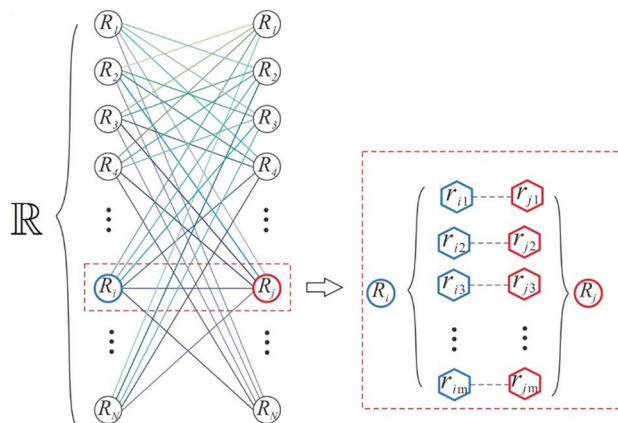


Fig. 7 Schematic figure of the quantification of the joint roughness heterogeneity

where $h = N(N - 1)/2$ is the number of all the combinations of any two individual samples in \mathbb{R} ; \mathbb{R} is the population of joint roughness vectors; and r_{ik} and r_{jk} indicate the roughness parameters of R_i and R_j in orientation k ($1 \leq k \leq m$). The schematic figure is shown in Fig. 7.

The determination of the sample number is a significant issue in the sampling survey (Murthy 1967). We suppose that n individual samples are selected from a population of N . Let the joint roughness at different positions be denoted by JRC_1 , JRC_2 , and JRC_i . On the basis of the partition sampling method, the joint roughness heterogeneity is indicated by the expected value $\hat{\theta}$, which is given as follows:

$$\hat{\theta} \sim N(\theta, V(\hat{\theta})). \tag{5}$$

The population parameter θ is given as follows:

$$\theta = \frac{1}{N} \sum_{i=1}^N JRC_i. \tag{6}$$

The accuracy of the estimation of population parameter θ is usually defined by the absolute error d or the margin of error r . The margin of error statistically expresses the random sampling error in a survey’s results, and it shows how close the sample’s results are to those when the entire population has been sampled. To ensure the accuracy of the estimation with confidence $1-\alpha$, the difference between the expected value $\hat{\theta}$ and the population parameter θ should be within the error, which is expressed as follows:

$$P\left(|\hat{\theta} - \theta| \leq d\right) = 1 - \alpha, \tag{7}$$

$$P\left(\frac{|\hat{\theta} - \theta|}{\theta} \leq r\right) = 1 - \alpha. \tag{8}$$

Based on the statistical measurement results in previous studies (Du 1999; Tanyas and Ulusay 2013; Ye et al. 2016), the result of the JRC values is an approximate normal distribution when the sample number exceeds 30. Thereafter, we can obtain the following:

$$P\left(\frac{|\hat{\theta} - \theta|}{\sqrt{V(\hat{\theta})}} \leq t\right) = 1 - \alpha, \tag{9}$$

where $V(\hat{\theta})$ is the sampling variance and t is the bilateral quantile of the standard normal distribution under a confidence level of $1-\alpha$. For instance, t equals 1.96 when $\alpha=0.05$.

The absolute error d and $V(\hat{\theta})$ can be expressed as follows:

$$d = t\sqrt{V(\hat{\theta})}, \tag{10}$$

$$V(\hat{\theta}) = \left(1 - \frac{n}{N}\right) \frac{S^2}{n}, \tag{11}$$

where S is the standard deviation of the population, N is the number of all samples extracted from different locations of a given rock joint, and n is the number of samples obtained by the partition sampling method.

Based on Eqs. (10) and (11), the effective sample number n_0 under a confidence level of $1-\alpha$ is given as follows:

$$n_0 = \frac{Nt^2S^2}{Nd^2 + t^2S^2} = \frac{Nt^2S^2}{Nr^2\theta^2 + t^2S^2}. \tag{12}$$

For instance, we can obtain all individual samples of 400 mm-long samples on the original profile using the global search method. The number of samples can be calculated by Eq. (1), as follows:

$$N = \frac{1000 - 400}{0.5} + 1 = 1201.$$

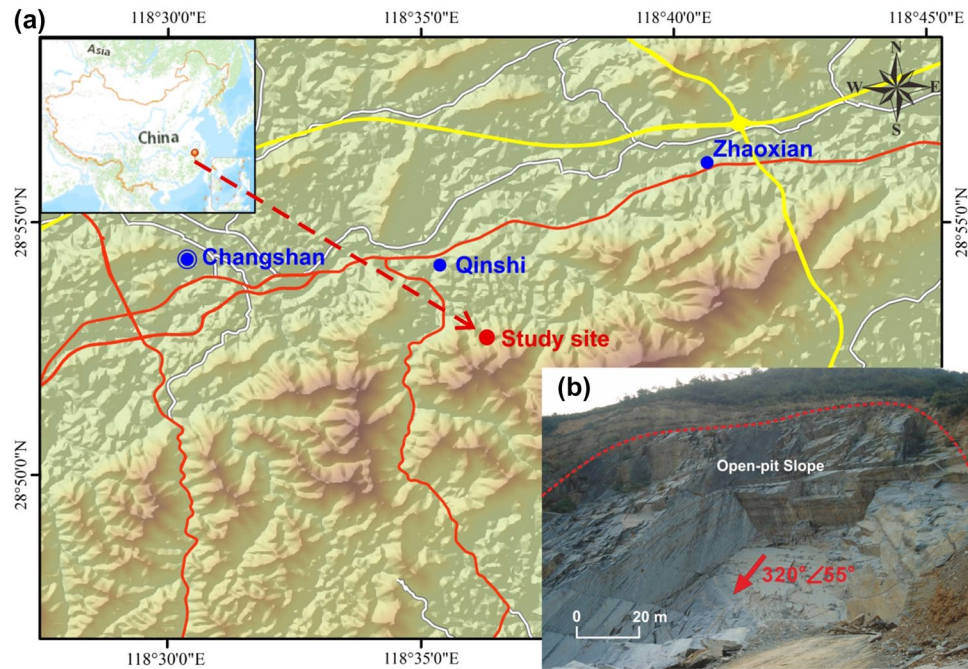
Then, statistical analysis was performed based on the JRC values of the obtained 400-mm-long samples, and the population parameter ($\theta=7.49$) and standard deviation ($S=1.42$) were determined. If the confidence level is 95% and the margin of error r is 5%, then the effective sample number is calculated as follows:

$$n_0 = \frac{Nt^2S^2}{Nr^2\theta^2 + t^2S^2} = \frac{1201 \times 1.96^2 \times 1.42^2}{1201 \times 0.05^2 \times 7.49^2 + 1.96^2 \times 1.42^2} = 52.8.$$

Table 1 Back-calculated margins of error based on different sampling methods

Method	Sample number	Confidence level (%)	Error (%)	Confidence level (%)	Error (%)	Confidence level (%)	Error (%)
Simple random sampling method	1	99.0	48.9	95.0	37.1	90.0	31.3
Processive magnifying sampling method	1		48.9		37.1		31.3
Partition sampling method	10		15.4		11.7		9.8

Fig. 8 Sites selected for the investigation. **a** Location map of the study site; **b** view of the structurally controlled open-pit slope



Thus, the sample number needed to statistically describe the roughness should exceed 53. This finding challenges the number of samples obtained by the partition sampling method.

Based on the partition sampling method, n ($n = L/l$) individual samples can be attained by the equal partition of the joint profile. On the basis of Eq. (12), the back-calculated margins of error attained using different methods are tabulated in Table 1. The margins of error obtained using the simple random sampling method or the processive magnifying sampling method range from 31.3 to 48.9% with a confidence level from 90 to 99%. The partition sampling method has a margin of error in the range from 9.8 to 15.4%. The samples obtained using the partition sampling method are more representative than the samples selected using the simple random sampling method or the processive magnifying sampling method, but estimation errors consistently arise due to inferences about the population based on observations of part of it. The margin of error is commonly taken as 5% for engineering practice (Yong et al. 2018c). The obtained margin of error using the partition sampling method is comparatively larger. Thus, it is inadequate to use the expected value $\hat{\theta}$ obtained using the partition sampling method to represent the population parameter θ . The global search method can be applied to analyze the roughness heterogeneity in the population to solve the sampling problem.

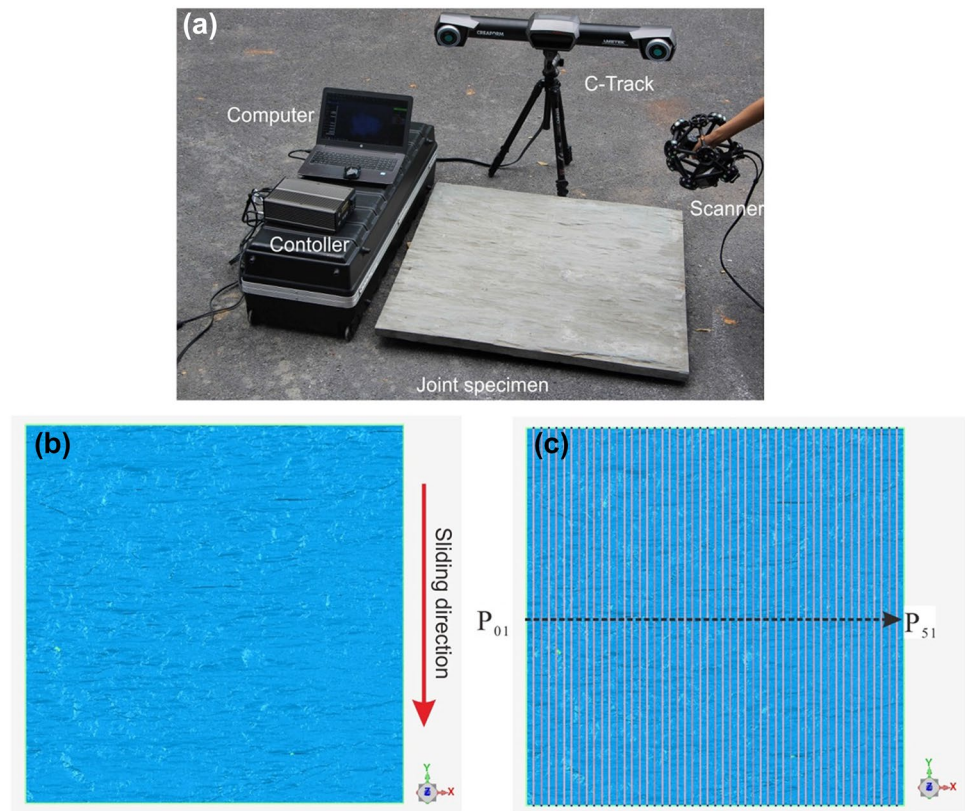
4 Rock Joint Sample and Roughness Measurements

4.1 Joint Selection and Description

The Heshangnong quarry is located at Qingshi Town, southeast of Changshan County, Zhejiang Province, China, approximately 213.5 km from Hangzhou city as shown in Fig. 8a. The exploitation of this quarry requires a pit with a length of 87 m, a width of 59 m and a maximum height of 79 m. In this pit, the overburden mainly consists of calcareous slate (Fig. 8b), which originated from Ordovician argillaceous limestone under the condition of light metamorphism. The stability of this open pit is controlled by the slate foliation, which generally dips approximately 55° to the NW. The grayish-green slate rock wall is foliated, very fine grained, and formed by the metamorphosis of intermediate tuff. The very distinct, continuous foliation planes in the overburden rock are oriented with strikes approximately parallel to the pit walls and dips towards the bottom of the pit (Fig. 8b).

The roughness parameters of rock joints are usually scale-dependent, but the scale dependency of joint roughness is limited to a certain size, defined as the stationarity threshold. The change in the roughness parameter is not visible for sample sizes greater than the stationarity threshold. To determine the morphological and mechanical properties of rock joints at laboratory and field scales, the size of the samples should be equal to or larger than the stationary

Fig. 9 Generation of the joint surface digitization. **a** Scanning of the joint surface. **b** Digitized joint surface. **c** Locations of the digitized profiles



threshold (Fardin 2007). Following the stationary threshold size mentioned in previous studies (Fardin et al. 2004; Tatone and Grasselli 2013), a sample with an overall area of $1100 \times 1100 \text{ mm}^2$ (Fig. 9a) was sawed from the slate rock and transported to the laboratory. A study area with a size of $1000 \times 1000 \text{ mm}^2$ was obtained from the center to avoid damage had occurred while in transit to the laboratory.

4.2 Digitization of the Joint Surface

A 3D laser scanning system, MetraScan 750 (Fig. 9a), with a maximum accuracy of 0.030 mm, was used to measure the geometry of the joint surface, and its main components include a scanner, C-Track cameras, a controller, and a computer. The surface acquisition was solved by observing the laser lines projected on the rock joint surface. As the laser swept over the surface by the scanner, the scanner measured the 3D coordinates of the sample surface using seven laser crosses, and the data were registered depending on the triangulated position. The final 3D surface model of the study area was obtained following point cloud data processing using the scanner software (Fig. 9b). We obtained 51 cross-sectional profiles along the potential shearing direction (Fig. 9c), namely, P_{01} , P_{02} , ..., and P_{51} . These profiles were digitized at a sampling interval (SI) of 0.5 mm, as this value

is often applied in previous studies (Li and Zhang 2015; Tatone and Grasselli 2010; Yong et al. 2018c).

4.3 Quantification of Joint Roughness

In this study, empirical, statistical, and fractal roughness parameters were used to describe the geometric irregularities of rock joints.

First, JRC, the most commonly used empirical roughness parameter, was taken to quantify the joint roughness. For field estimation purposes, the JRC values can be approximately determined based on the relations between the JRC and the maximum profile amplitude (A_{\max}) measured over a sample length (L) (Barton 1981; Palmström 1995). The relation between the JRC and the undulation factor u ($u = A_{\max}/L$) can be used to evaluate the scale effects on the JRC. Yong et al. (2018a) proposed a programmed method for determining the A_{\max} of digitized joint profiles. As shown in Fig. 10, the main process of determining A_{\max} is introduced as follows:

Step 1: Arbitrarily select two points from the digitized profile (x_p, y_p) , (x_q, y_q) .

Step 2: Obtain the linear equation of the line passing through (x_p, y_p) , (x_q, y_q) as follows:

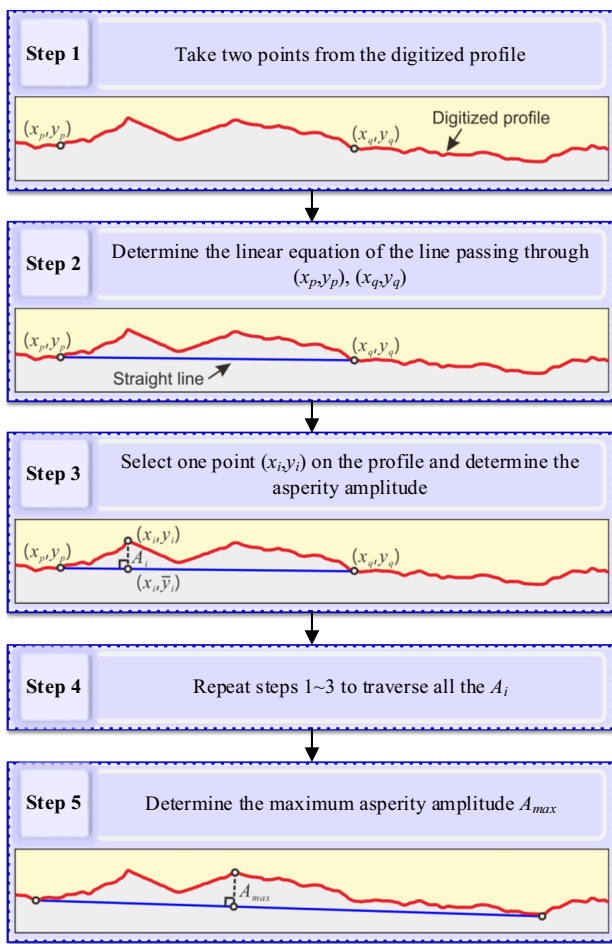


Fig. 10 Flowchart illustrating the steps involved in determining A_{max}

$$\bar{y} = \frac{y_p - y_q}{x_p - x_q}(x - x_p) + y_p. \tag{13}$$

Step 3: Select another point (x_i, y_i) on the digitized profile, where $x_i \in (x_p, x_q)$. Then, determine the asperity amplitude by calculating the normal distance from this point to the line as follows:

$$A = \frac{\left| \frac{y_p - y_q}{x_p - x_q}(x_i - x_p) + y_p - y_i \right|}{\sqrt{1 + \left(\frac{y_p - y_q}{x_p - x_q} \right)^2}}. \tag{14}$$

Step 4: According to steps (1) to (3), an iterative process was used to determine the asperity amplitudes, by changing the points (x_p, y_p) , (x_q, y_q) and (x_0, y_0) , which took into account all possible combinations of these three points from the digitized profile.

Step 5: The maximum asperity amplitude A_{max} was determined by finding the maximum value of A .

Based on the results, the joint roughness coefficient based on Barton's straight edge method (Barton 1981; Yong et al. 2018a) is as follows:

$$JRC_n = 400 \frac{A_{max}}{L_n}. \tag{15}$$

In addition, four widely accepted statistical parameters were selected to investigate the joint roughness heterogeneity. The following three parameters are used to quantify of 2D joint roughness: the first-derivative root-mean-square Z_2 (Tse and Cruden 1979), the roughness profile index or profile sinuosity R_p (Maerz et al. 1990), and the modified root-mean-square

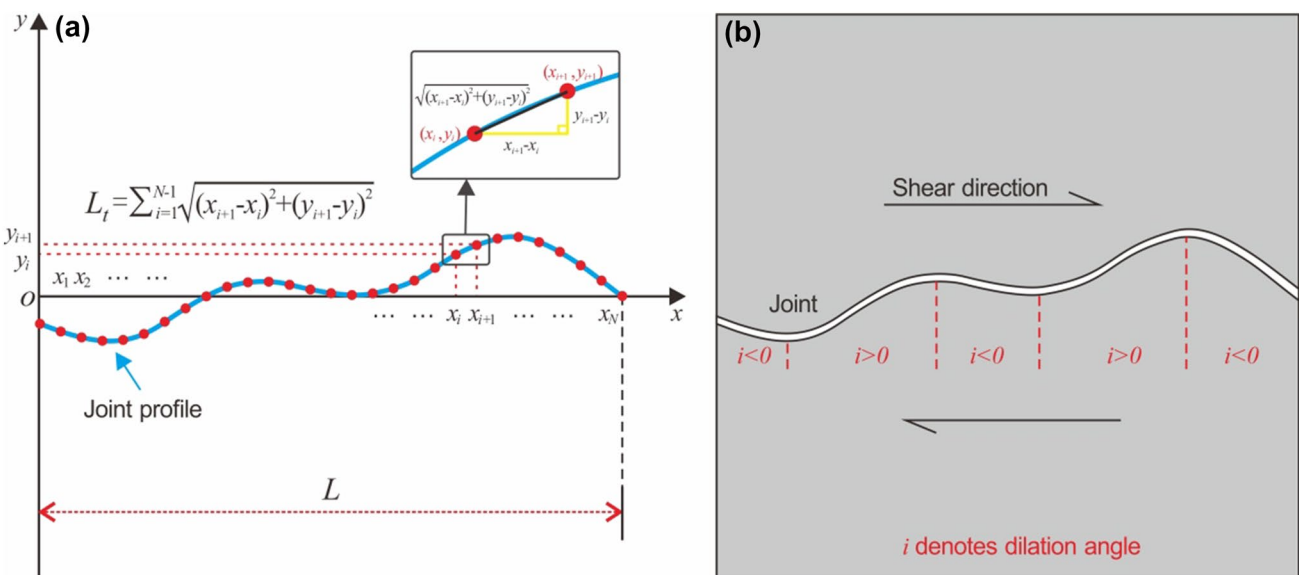


Fig. 11 Variation of inclination angles along a rock joint profile (Zhang et al. 2014)

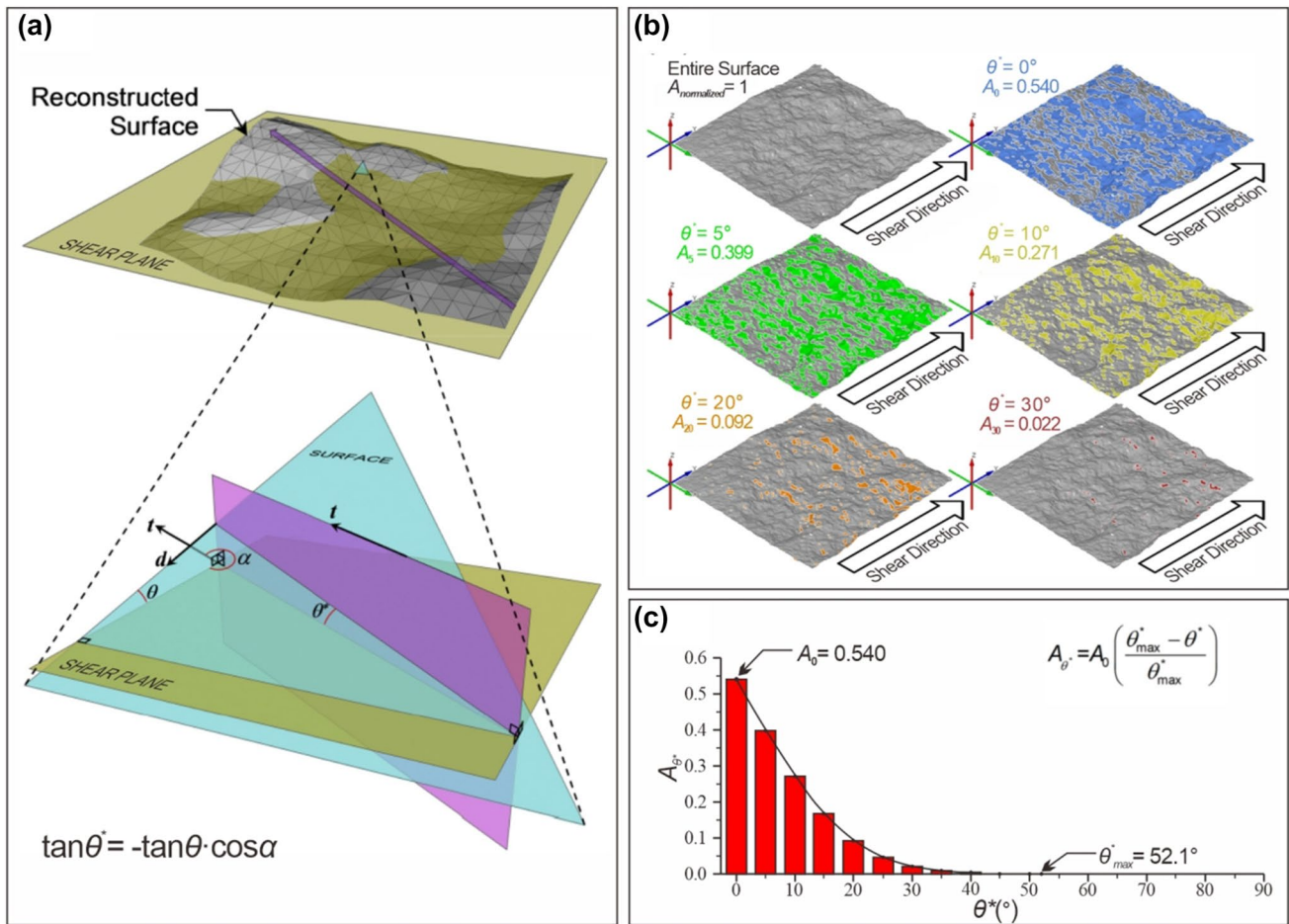


Fig. 12 Schematic figure showing the definition of the roughness metrics $\theta_{max}^*/[C + 1]_{3D}$ (Tatone and Grasselli 2009). **a** Sketch of the apparent dip angle θ^* . **b** Schematic diagram illustrating the use of the

angular threshold concept to determine A_{θ^*} . **c** Cumulative distribution of A_{θ^*} as a function of θ^*

Z_2' (Zhang et al. 2017). The first-derivative root-mean-square Z_2 and the roughness profile index or profile sinuosity R_p are common roughness parameters, and they can be determined by the following equations:

$$Z_2 = \sqrt{\frac{1}{L} \int_{x=0}^{x=L} \left(\frac{dy}{dx} \right)^2 dx} \approx \sqrt{\frac{1}{N} \sum_{i=1}^{N-1} \left[\frac{(y_{i+1} - y_i)}{(x_{i+1} - x_i)} \right]^2} \tag{16}$$

$$R_p = \frac{L_t}{L} = \frac{\sum_{i=1}^{N-1} \sqrt{(x_{i+1} - x_i)^2 + (y_{i+1} - y_i)^2}}{L}, \tag{17}$$

where x and y are the horizontal and vertical coordinates of the points along a profile; (x_{i+1}, y_{i+1}) and (x_i, y_i) represent the adjacent coordinates of a profile; N is the number of measured points over a profile; L_t is the true length of the profile, which refers to the sum of the lengths of the lines

between two adjacent points; and L is the length of the profile projected on the x -axis (see Fig. 11a).

Zhang et al. (2014) found that the results of shear box tests in forward and reverse directions were different, which indicated that roughness was also different in forward and reverse directions. To account for the directional dependencies, they classified the dilation angles into positive and negative angles (see Fig. 11b) and suggested that only positive angles should be considered in the process of determining joint roughness. Based on Eq. (16), Zhang et al. (2014) defined the modified root-mean-square Z_2' as follows:

$$Z_2' = \sqrt{\frac{1}{L} \int_{x=0}^{x=L} \left(\max \left(0, \frac{dy}{dx} \right) \right)^2 dx} = \left[\sum_{i=1}^{N-1} \frac{(\max(0, y_{i+1} - y_i))^2}{(x_{i+1} - x_i)L} \right]^{1/2}. \tag{18}$$

In this study, the roughness metric $\theta_{\max}^*/[C + 1]_{3D}$ (Grasselli et al. 2002) was used to characterize the 3D joint roughness. Grasselli (2001) found that only the parts of the joint surface that face the shear direction and are steeper than a threshold inclination provide shear resistance. Then, he developed the roughness metric $\theta_{\max}^*/[C + 1]_{3D}$ based on an angular threshold concept, and this parameter was initially developed to identify potential contact areas during direct shear testing of rock joints.

As shown in Fig. 12a, the joint surface is discretized into adjacent triangles. Each triangle orientation is uniquely identified by its azimuth angle α and dip angle θ . Azimuth angle α is the angle between the true dip vector d projected on the shear plane and the shear vector t , measured clockwise from t . Dip angle θ is the angle between the shear plane and the triangle. As presented in detail by Grasselli et al. (2002) and Grasselli (2006), the apparent dip angle θ^* describes the apparent inclination of each triangle with respect to the shear direction, and it is obtained by projecting the dip angle along the vertical plane which contains the shear direction, as follows:

$$\tan \theta^* = -\tan \theta \cdot \cos \alpha. \quad (19)$$

For each surface, it is possible to calculate the area of the joint that has an apparent dip angle equal to or greater than a chosen threshold dip angle, which represents the area in contact or damaged during shearing (Grasselli, 2006). As shown in Fig. 12b, the areas that are steeper than a certain value of θ^* are highlighted on the entire surface. The ratio of the areas steeper than a threshold dip angle to the area of the entire surface is denoted by A_{θ^*} . For example, the areas that are steeper than a threshold dip angle ($\theta^* = 0$) are highlighted in blue color, and the ratio A_{θ^*} of the highlighted area to the entire surface is 0.540. As shown in Fig. 12b, when the values of θ^* equal to 0° , 5° , 10° , 20° , and 30° are considered, the corresponding values of A_{θ^*} are 0.540, 0.399, 0.271, 0.092, and 0.022, respectively.

By varying the θ^* from 0° to the maximum apparent dip angle θ_{\max}^* , the ratios A_{θ^*} were obtained. Figure 12c shows the relationship between A_{θ^*} and θ^* . It is possible to plot the variation of θ^* as a function of the threshold dip angle, and their relationship can be expressed in terms of Tatone and Grasselli (2010)'s equation:

$$A_{\theta^*} = A_0 \left(\frac{\theta_{\max}^* - \theta^*}{\theta_{\max}^*} \right)^C, \quad (20)$$

where A_0 is the total potential contact area ratio when $\theta^* = 0^\circ$; C is the dimensionless empirical fitting parameter calculated via non-linear least-squares regression.

Then, the roughness metric $\theta_{\max}^*/[C + 1]_{3D}$ can be calculated based on the obtained parameters θ_{\max}^* and C . In

addition, Tatone and Grasselli (2010) expand the application of the roughness metric and proposed a new parameter $\theta_{\max}^*/[C + 1]_{2D}$ for the characterization of 2D roughness. In this work, this parameter was also used to quantify the roughness of joint profiles.

Furthermore, the fractal dimensions D of a rock joint profile were calculated using the compass-walking method, which is also a widely accepted parameter for quantifying the roughness of a natural rock joint profile (Li and Zhang 2015).

5 Measurement Results and Analysis

5.1 Heterogeneity of Joint Roughness by Different Roughness Parameters

The original joint profile P_{01} is applied here as an example (Fig. 13a), the global search method was applied to investigate the roughness heterogeneity in situation A. Profile P_{01} is 1000 mm long. Based on the partition sampling method, this profile can be equally separated into ten 100 mm subsections (Fig. 13b). The number of the samples obtained is $n = 10$. Based on the global search method, the samples were taken from different positions on the original profile by moving an SI distance each time (Fig. 13c). The total number N of subsections is 1801 based on Eq. (1).

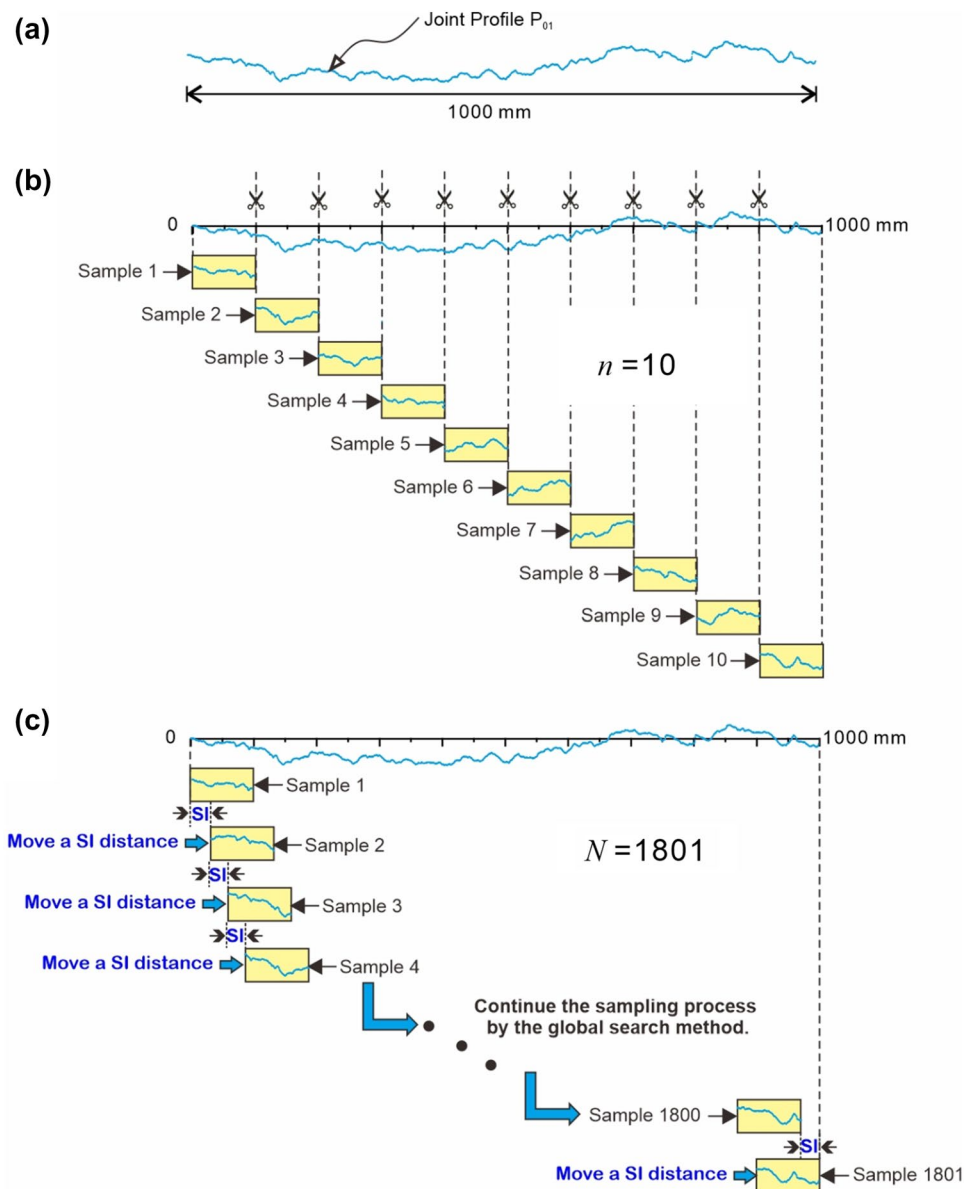
The joint roughness parameters of all the individual samples in the roughness population obtained by the global search method are displayed in the histograms in Fig. 14. The frequency histograms of the roughness parameters indicate the joint roughness heterogeneity. We can evaluate the joint roughness heterogeneity by Eq. (4). In this study, the roughness of the joint was quantified by empirical, statistical, and fractal roughness parameters. To ease the comparison between the roughness heterogeneity by different parameters, all the roughness parameters were normalized into a range between 1 and 2 before calculating the roughness heterogeneity. The normalized values r_i of the roughness parameters are obtained using the following equation:

$$r_i = \frac{J_i^* - J_{\min}^*}{J_{\max}^* - J_{\min}^*} + 1, \quad (21)$$

where J_i^* is a roughness parameter which can be JRC, Z_2 , R_p , Z_2' , $\theta_{\max}^*/[C + 1]_{2D}$, and D . J_{\min}^* and J_{\max}^* are the minimum and maximum values of the roughness parameters, respectively.

The ratio of heterogeneity ($H \geq 1$) indicates the overall difference between the roughness of the samples taken from different positions. When the ratio equals 1, it reflects that the joint surface roughness is homogeneous. Larger ratios indicate more noticeable differences in the roughness of

Fig. 13 Schematic diagrams of the sampling results. **a** The original joint profile P_{01} . **b** Partition sampling method. **c** Global search method



samples collected from various positions. According to the obtained normalized values of different roughness parameters, the heterogeneity ratios H were calculated using Eq. (4). The heterogeneity ratios H for JRC , Z_2 , R_p , Z_2' , $\theta_{max}^*/[C + 1]_{2D}$, and D were 1.051, 1.050, 1.050, 1.059, 1.047, and 1.046, respectively. This result indicates that different roughness estimation methods produce close evaluations of the heterogeneity.

5.2 Error in Joint Roughness Heterogeneity Estimated by the Partition Sampling Method

In previous studies, JRC is the most commonly used parameter for quantifying the joint roughness, because it provides insights into the shear strength and deformation behavior of

rock joints (Morelli 2014). Here, it was taken to study the error in the joint roughness heterogeneity estimate by the partition sampling method.

Figure 15a is the frequency histogram of the JRC values of the samples obtained using the global search method. A normal distribution is shown here with a mean value θ of 13.34 and a standard deviation S of 3.40. Taking into account the fact that all samples in the population can be obtained by the global search method, θ is the population parameter. However, the JRC values of the samples obtained using the partition sampling method do not follow a normal distribution (Fig. 15b). Compared with the statistical results obtained by the global search method, the expected value $\hat{\theta}$ obtained using the partition sampling method is close to the population parameter θ , but the standard deviation \hat{S}

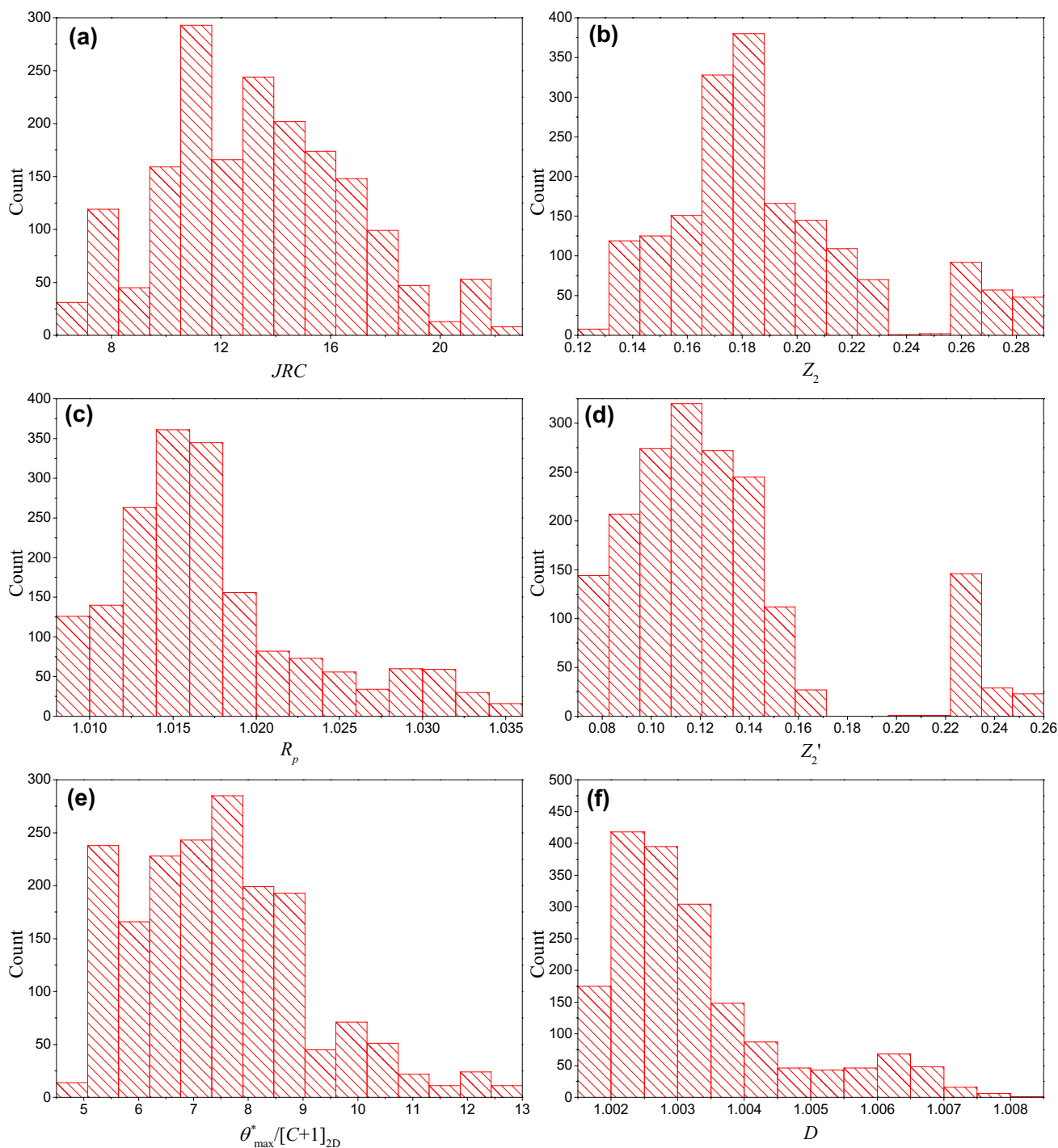


Fig. 14 Histograms of the heterogeneity of joint roughness using different roughness parameters. **a** JRC, **b** Z_2 , **c** R_p , **d** Z_2' , **e** $\theta_{\max}^*/[C + 1]_{2D}$, **f** D

obtained using the partition sampling method is distinctly different from S . In addition, the roughness distribution obtained using the partition sampling method (Fig. 15b) is inconsistent with the result obtained using the global search method (Fig. 15a). For example, the JRC values in the ranges from 12 to 14 and from 18 to 20 are missing in Fig. 15b. However, the JRC values range from 12 to 14 with highest

relative frequency (Fig. 15a). Therefore, the distinct differences in the standard deviation and roughness distribution indicate that the statistical results based on the partition sampling method may introduce estimation errors.

In addition, we can evaluate whether the sample number is sufficient based on Eq. (12). Under a confidence level

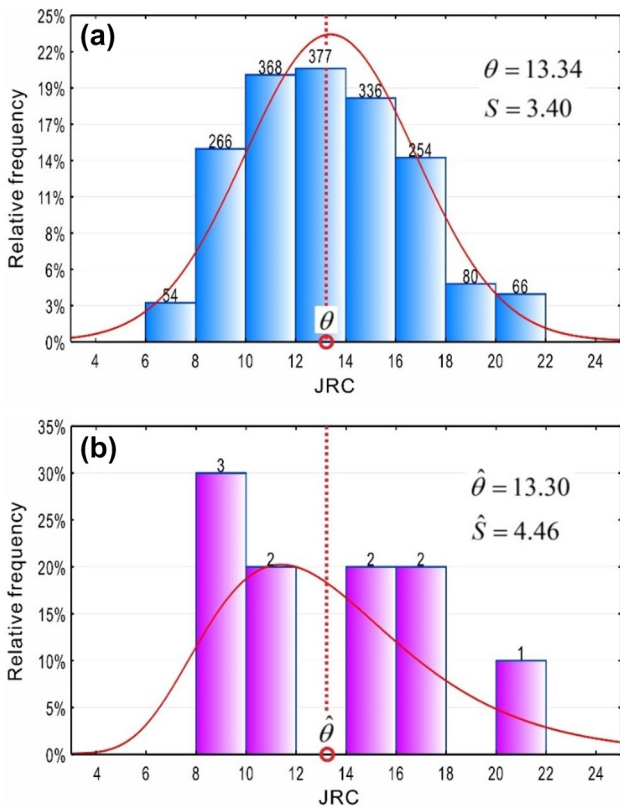


Fig. 15 Comparison of the JRC values of 100 mm joint samples. **a** Histograms that show the distribution of the JRC values using the global search method. **b** Histograms that show the distribution of the JRC values using partition sampling method

of 95% and a margin of error of 10%, the effective sample number is calculated using Eq. (12) as follows:

$$n_0 = \frac{Nr^2S^2}{Nr^2\theta^2 + r^2S^2} = \frac{1801 \times 1.96^2 \times 3.40^2}{1801 \times 0.1^2 \times 13.34^2 + 1.96^2 \times 3.40^2} \approx 25.$$

Only ten samples can be obtained by the partition sampling method. This number is less than n_0 . Thus, the sample number suggested by the partition sampling method is insufficient. Furthermore, only one sample could be obtained based on the simple random sampling method and the processive magnifying sampling method. It is smaller than the sample number by the partition sampling method, thus it is also insufficient. In statistics, the margin of error is a statistic expressing the amount of random sampling error in the results of a survey. It indicates how far the results deviate from the real population value. We can calculate the margin of error by Eq. (12) for a confidence level of 95%. The back-calculated margins for the partition sampling method, the simple random sampling method and the processive magnifying sampling method are 15.75%, 49.9% and 49.9%, respectively. The margin of error obtained using these traditional sampling methods is greater than 10%. Therefore, the roughness parameters of the samples obtained by these conventional sampling methods are not representative of the overall roughness.

For each joint profile with length of 1000 mm, we can obtain ten joint samples with the length of 100 mm or two samples with the length of 500 mm using the partition sampling method. As previously mentioned, these ten samples obtained by the partition sampling method are insufficient for the statistical analysis of the roughness of the 100 mm joint samples. The 500 mm samples were obtained from

Fig. 16 Comparison of the JRC values of 500-mm-long joint samples based on partition sampling method and global search method. **a** The mean values and **b** the standard deviations

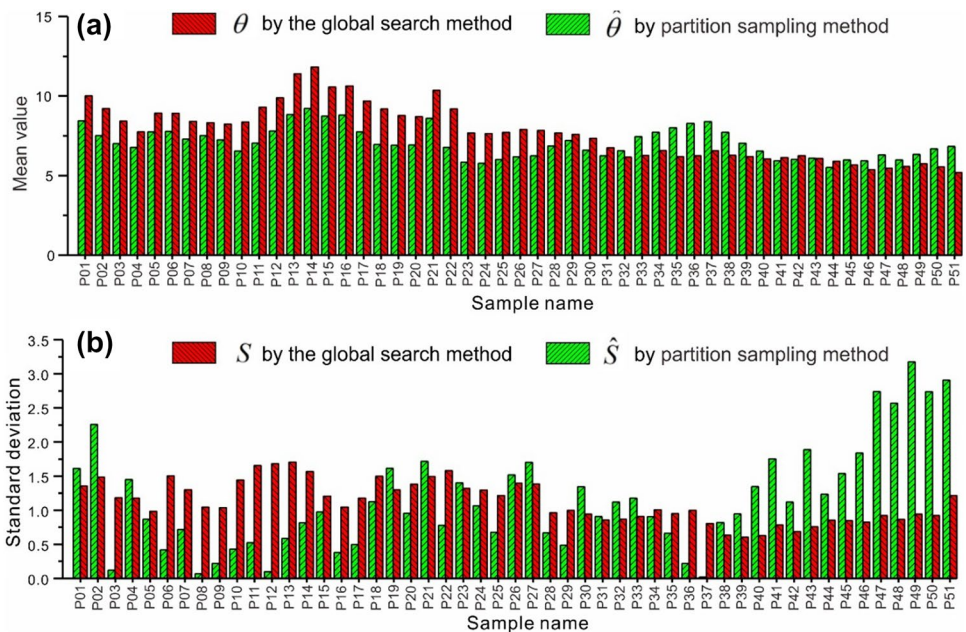
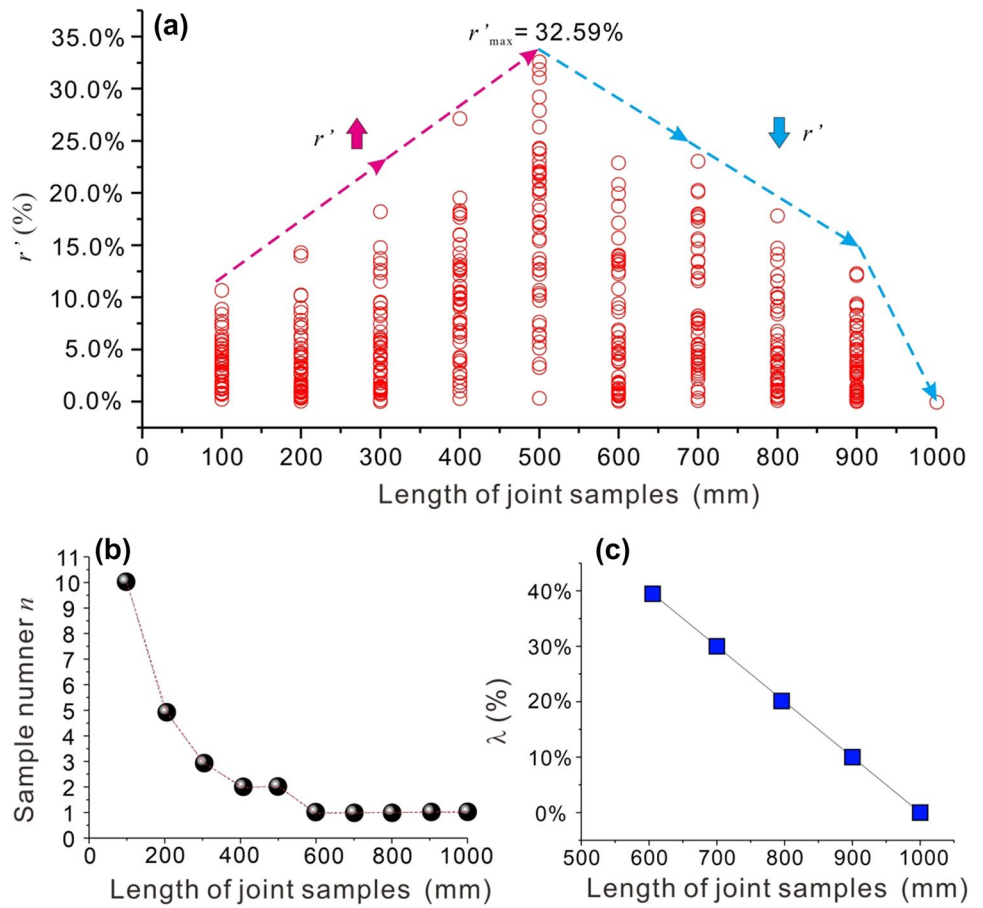


Fig. 17 Comparison between the population value θ by the global search method and the expected value $\hat{\theta}$ by the partition sampling method. **a** Variation in the relative errors with the length of the joint samples. **b** The change in the sample number. **c** The change in the percentage of the neglected length



the profiles ($P_{01}, P_{02}, \dots,$ and P_{51}) in Fig. 9 using the partition sampling method. First, the joint samples were obtained from the profiles ($P_{01}, P_{02}, \dots,$ and P_{51}) in Fig. 9 using the partition sampling method. Then, the expected value $\hat{\theta}$ and standard deviations \hat{S} of the samples taken from each profile were calculated. Figure 16 illustrates that the mean values and standard deviations present apparent differences between the values obtained by the global search method and the partition sampling method. For each profile, different samples can be extracted from different locations using the global search method, and the total number of the samples is 1001 based on Eq. (1). Based on the global search method, the heterogeneity of rock joints was characterized by the roughness of all individual samples. However, only two samples can be extracted from each profile using the partition sampling method. The heterogeneity estimated by the partition sampling method may be biased because of the insufficient samples. As shown in Fig. 16a, the expected values ($\hat{\theta}$) of the samples obtained from the profiles P_{01} to P_{31} are underestimated, but the $\hat{\theta}$ values of the samples obtained from the profiles P_{32} to P_{51} are overestimated. The largest relative error between $\hat{\theta}$ and θ is 32.59%. Figure 16b shows

a comparison of the standard deviations of the JRC values based on the partition sampling method and the global search method. For the partition sampling method, the standard deviation \hat{S} is a measure of the variation between the roughness of the two samples, which cannot reflect the variations between the roughness of samples taken from various locations. The differences between \hat{S} and S are greater than the difference between $\hat{\theta}$ and θ , and the largest relative error between \hat{S} and S is 236.34%. Therefore, the expected values $\hat{\theta}$ of 500 mm joint samples by the partition sampling method also failed to represent the overall roughness.

The difference between the population value θ by the global search method and the expected value $\hat{\theta}$ by the partition sampling method can be quantified by the absolute values of the relative errors r' , as follows:

$$r' = \frac{|\theta - \hat{\theta}|}{\theta} \times 100\%. \tag{22}$$

As shown in Fig. 17a, the relative errors r' of the joint profiles ($P_{01}, P_{02}, \dots,$ and P_{51}) were calculated. It was validated that the differences between the results by the global search method and the partition sampling method not only

vary from fracture to fracture but also vary with scale. The distribution of the relative error r' can be divided into two sections. For the first section, the length of the samples does not exceed 500 mm, the maximum value of the relative error r' increases with the sample length, and the overall maximum value is 32.59%. For the second section, the sample length is larger than 500 mm, and the maximum value of the relative error r' decreases with the sample length. In the first section, the increasing trend of the maximum value of the relative error r' is due to the reduction in the number of samples of each length (Fig. 17b). For the 100-mm-long samples, 10 samples can be obtained using the partition sampling method, while only 2 samples can be obtained for the 400-mm- and 500-mm-long samples. In the second section, the decreasing trend of the relative error r' is due to the changes in the abandoned part generated by the partition sampling method. For a 600 mm sample, the length of the abandoned part is 400 mm, so the percentage of the abandoned length λ is 40%. The roughness of the obtained 600 mm sample can only represent the roughness characteristics of the joint in the first 600 mm of length. Then, the percentage of the abandoned length λ decreases as the sample length increases (Fig. 17c), which contributes to the decreasing trend of the relative error r' .

5.3 Applications for Searching Representative Samples

Surveying the shear behavior requires an understanding of all the potential sampling errors that can bias the result. Roughness heterogeneity as an efficient indicator of shear behavior may be used to explore representative test samples. Yong et al. (2018b) suggested that a representative sample can be obtained by finding the sample whose roughness is close to the maximum-likelihood estimation of the roughness probability distributions. Here, the representative samples were obtained based on the roughness probability distributions of the joint samples with the same size. The representativeness of each sample can be evaluated by the following:

$$\eta_i = \frac{|JRC_i - \theta|}{\theta} \times 100\%, \tag{23}$$

where η_i is the representativeness coefficient; JRC_i denotes the JRC of joint sample i ; and θ is the mean value of the roughness of all samples obtained from different positions using the global search method.

The most representative sample of each size can be determined when η_i reaches the minimum value. Thereafter, the position of the sample can be determined on the profile, which can be selected for the scale effect study.

By taking the profile P_{01} as an example, the JRC values of the samples with the lengths of 100 mm to 1000 mm were obtained using the global search method. For the samples of 100 mm length, the mean value θ of the roughness of all samples obtained from different positions is 13.34. We calculated the representativeness of each sample with the length of 100 mm using Eq. (23) and found that η of joint sample taken from 779.5 to 879.5 mm on P_{01} reached the minimum value. That is, the location of the representative sample of a length of 100 mm ranges from 779.5 to 879.5 mm in the x-axial direction. Following the same process, we can determine the location of the representative samples at the lengths of 200 mm to 1000 mm. The positions of the representative samples of different sizes are shown in Fig. 18.

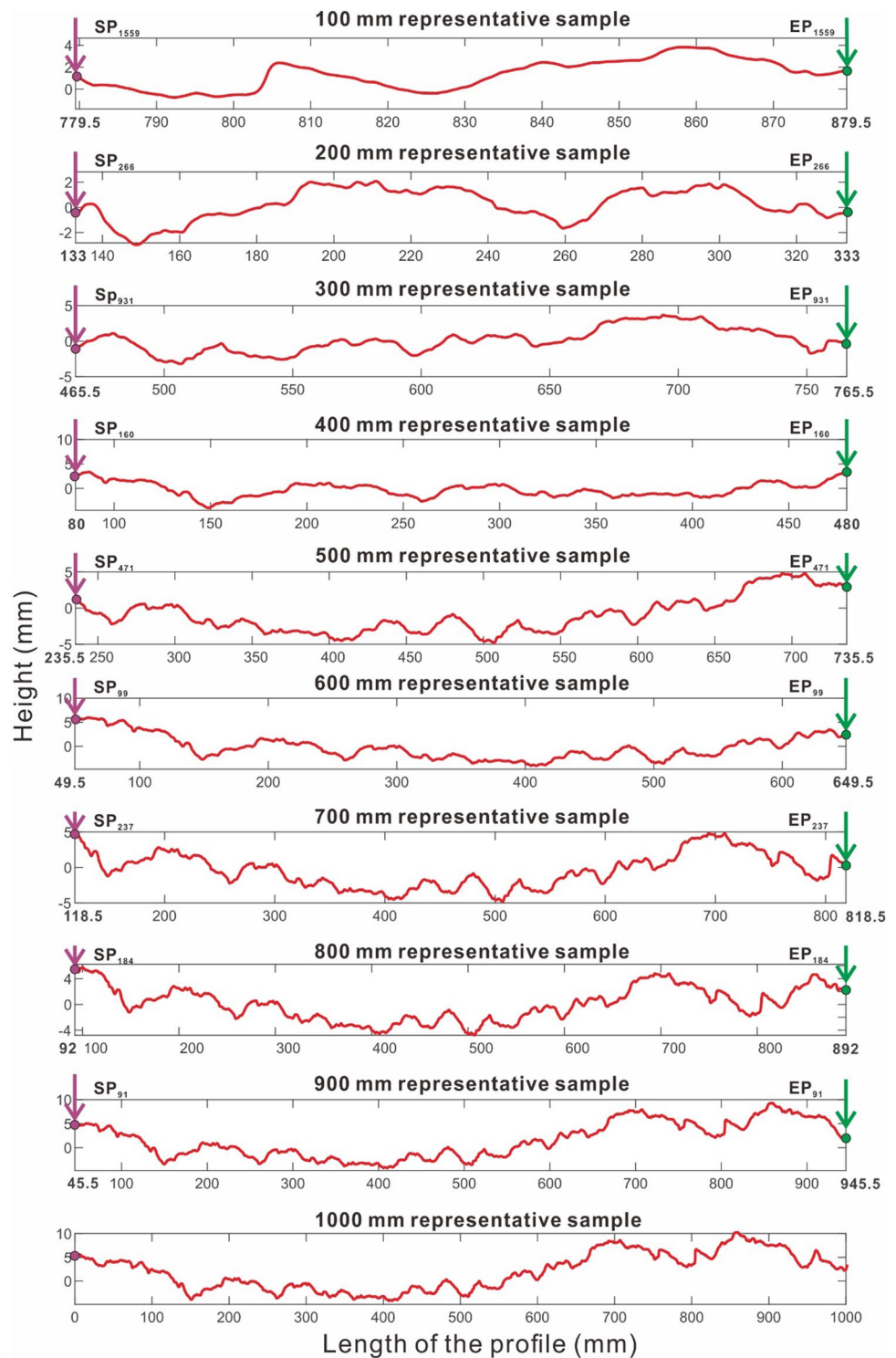
6 Heterogeneity of 3D Joint Roughness

Heterogeneity exists in both 2D profiles and 3D surface topographies (Du 1994). The heterogeneity of joint roughness was analyzed on the basis of the joint profiles in the aforementioned sections. Here, the heterogeneity of the 3D joint roughness was investigated based on joint samples with sizes of 100×100 mm² obtained from the digitized joint surface in Fig. 9.

Based on the global search method, independent roughness samples can be obtained by changing their positions, and a population of the roughness of all samples with a number of $(N = 1801)^2$ can be obtained. Although sampling error exists when using the partition sampling method, the error usually decreases with the sample number. A maximum error of 11.8% was observed in the heterogeneity of 2D profiles with sizes of 100 mm. The digitized joint surface can be divided into 100 samples using the partition sampling method (Fig. 19). The heterogeneity of 3D surfaces was approximately estimated based on the partition sampling method. As shown in Fig. 19, there is a distinct difference in the surface roughness of two adjacent samples S_{1-1} and S_{1-2} , as the topography of sample S_{1-2} fluctuates more than that of sample S_{1-1} . Samples S_{1-1} and S_{1-10} are obtained from the corners of the joint surface. The surface of sample S_{1-10} is comparatively smoother than that of sample S_{1-1} . The surface roughness of sample S_{5-5} is slightly rough, but the areas that face the shear direction are completely different from those of samples S_{1-1} and S_{1-10} . It is well known that surface roughness is one of the main factors affecting the shear strength of rock joints. Thus, the shear behaviors of samples S_{1-1} , S_{1-10} , and S_{5-5} are probably different.

As mentioned in Sect. 2, there are three situations of exposed potential sliding planes encountered in field surveys. The following two groups of 3D joint roughness samples were used to show the difference of heterogeneity in different situations: samples S_{1-1} , $S_{2-1} \dots S_{10-1}$ obtained in

Fig. 18 Sampling locations of representative samples based on the global search method



the direction perpendicular to the shear direction were taken as an example to show the heterogeneity of the samples in situation A, and samples S_{1-1} , S_{1-2} ... S_{1-10} obtained in the direction perpendicular to the shear direction were used to illustrate the heterogeneity in situation B. The former reflects the roughness diversity spread along the sliding direction,

and the latter reflects the diversity of surface roughness in the direction perpendicular to the sliding direction. The surface topographies of these samples were displayed in a contour plot to visualize the anisotropy of surface roughness. The surface topographies of the samples in Fig. 20a had greater variance. The differences in the topographies

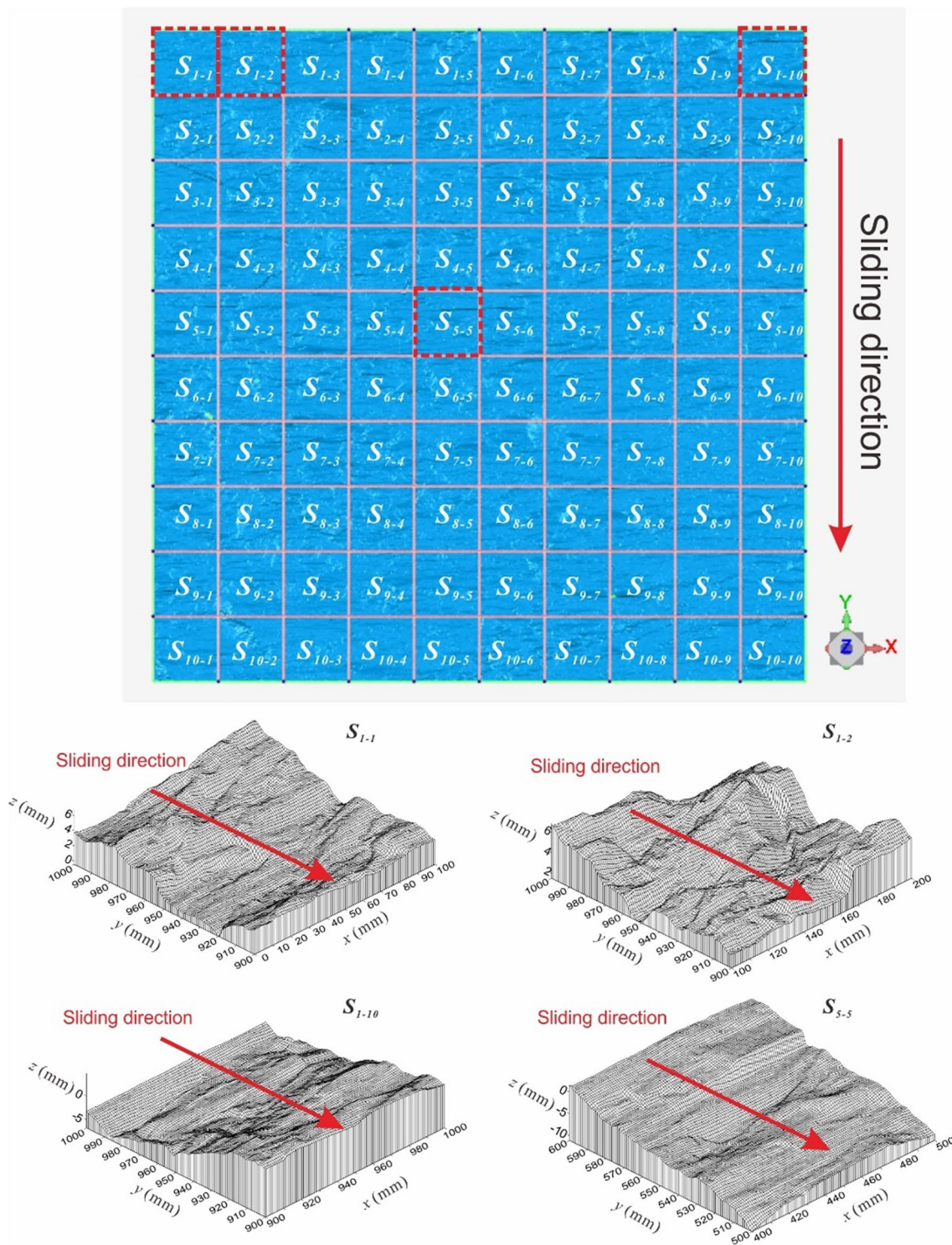


Fig. 19 3D joint roughness samples with sizes of $100 \times 100 \text{ mm}^2$

of each sample in Fig. 20b are less apparent. The values of the directional roughness $\theta_{\max}^*/[C + 1]_{3D}$ change with the locations of the joint samples in field situations A and B. In field situation A, the directions of the maximum and

minimum values of $\theta_{\max}^*/[C + 1]_{3D}$ change with the locations of the joint samples (Fig. 20c), but the directions of the maximum and minimum values are almost constant in field situation B (Fig. 20d). Using Eq. (4), the heterogeneity

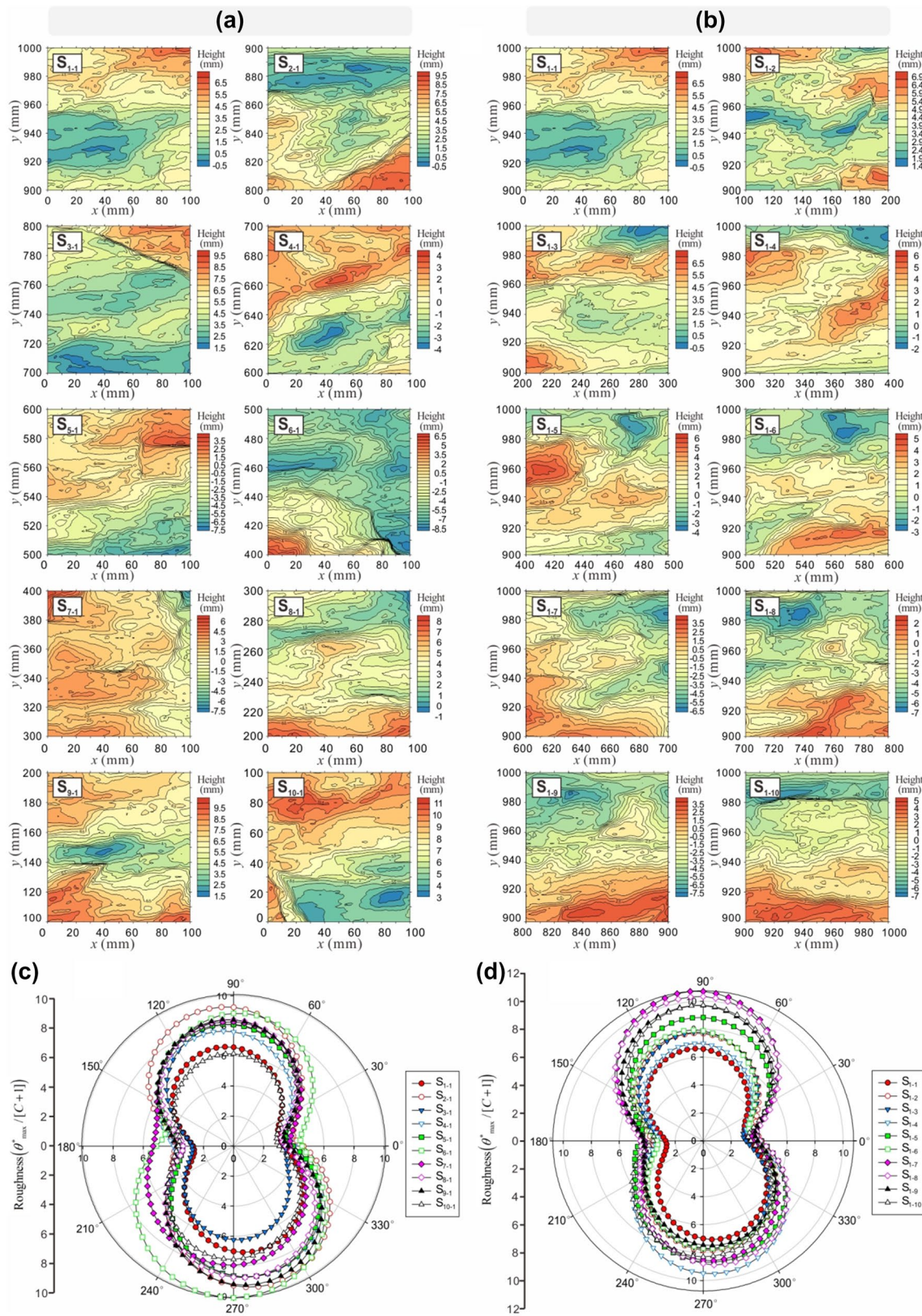


Fig. 20 Comparisons between the heterogeneities of the samples. **a** Contour plots of the surface topographies of the samples under field condition A. **b** Contour plots of surface topographies of the samples

under field condition B. **c** Polar plots of the 3D directional roughness surface of the samples in situation A. **d** Polar plots of the 3D directional roughness surface of the samples in situation B

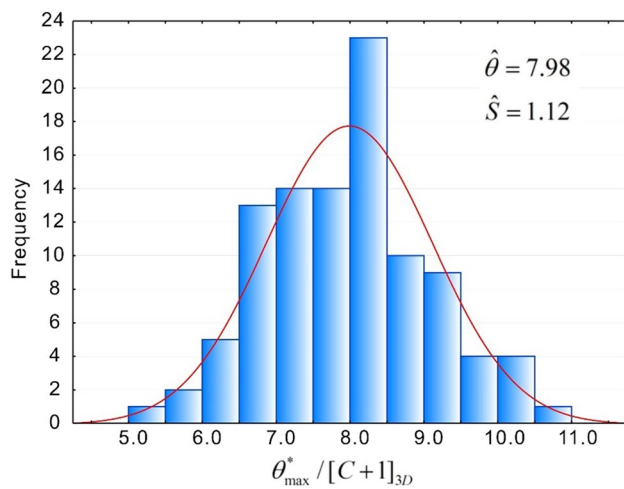


Fig. 21 Histogram of the 3D joint roughness along the sliding direction

ratio H in situation A is 1.046, and the result for situation B is 1.039. Thus, the heterogeneity of the 3D joint roughness is more apparent in situation A than in situation B.

The values of $\theta_{\max}^* / [C + 1]_{3D}$ along the sliding direction of all samples are shown in Fig. 21, which vary from 5.24 to 10.69. These data follow a normal distribution with a mean value of 7.98 and a standard deviation of 1.12. Here, the representative samples were achieved based on the $\theta_{\max}^* / [C + 1]_{3D}$ probability distributions of the joint samples. Sample $S_{4.3}$ was found to be a representative sample, whose roughness metric $\theta_{\max}^* / [C + 1]_{3D}$ is 8.08.

7 Conclusions

Roughness heterogeneity refers to the fact that joint roughness measurements vary with position, and it exists in both two-dimensional (2D) profiles and three-dimensional (3D) surface topographies. Little attention has been given to the influence of heterogeneity on joint roughness estimation in previous studies, and the problem regarding the inaccuracy of joint roughness estimation based on inadequate samples remains unsolved. According to the statistical analysis of the effective sample number, the roughness samples in conventional methods are normally insufficient to represent the overall roughness and the estimation error consistently arises in the characterization of the joint roughness heterogeneity.

A new method, namely the global search method, was proposed to characterize the heterogeneity of rock joints based on the analysis of the roughness of all individual samples. This method allows all independent samples within the populations to be obtained by changing the starting and end points, without abandoning any side sections of the original profile. This method is convenient for

acquiring a sufficient number of samples of various sizes and helpful for improving the determination of the scale effect. It was verified that the expected value obtained from conventional methods cannot represent the overall roughness of the joint profile. The proposed method is capable of systematically characterizing the heterogeneity of the roughness of rock joints of various sizes.

In the case study on the natural slate joint, the joint roughness heterogeneity was systematically investigated based on both 2D profiles and 3D surface topographies. The error in the estimation of joint roughness heterogeneity using the partition sampling method was analyzed. It illustrates that the maximum relative error between the population parameter and the expected value first increased with the length of the joint sample and then decreased when the sample length was exceeding the half of the length of the original profile. The characterization of joint roughness heterogeneity is applied for the exploration of representative samples. Representative samples were obtained by finding the sample whose roughness was closest to the population parameter of all individual samples.

Acknowledgements The study was funded by the National Natural Science Foundation of China (Nos. 42177117, 41427802, and 41572299), Zhejiang Provincial Natural Science Foundation (No. LQ16D020001), and Zhejiang Collaborative Innovation Center for Prevention and Control of Mountain Geological Hazards (Nos. PCMGH-2017-Z03, PCMGH-2017-Y-04, and PCMGH-2017-Y-05).

Declarations

Conflict of Interest The authors have no conflicts of interest to declare.

Open Access This article is licensed under a Creative Commons Attribution 4.0 International License, which permits use, sharing, adaptation, distribution and reproduction in any medium or format, as long as you give appropriate credit to the original author(s) and the source, provide a link to the Creative Commons licence, and indicate if changes were made. The images or other third party material in this article are included in the article's Creative Commons licence, unless indicated otherwise in a credit line to the material. If material is not included in the article's Creative Commons licence and your intended use is not permitted by statutory regulation or exceeds the permitted use, you will need to obtain permission directly from the copyright holder. To view a copy of this licence, visit <http://creativecommons.org/licenses/by/4.0/>.

References

- Alameda-Hernández P, Jiménez-Perálvarez J, Palenzuela JA, El Hamdouni R, Irigaray C, Cabrerizo MA, Chacón J (2014) Improvement of the JRC calculation using different parameters obtained through a new survey method applied to rock discontinuities. *Rock Mech Rock Eng* 47:2047–2060. <https://doi.org/10.1007/s00603-013-0532-2>
- Bae D-S, Kim K-S, Koh Y-K, Kim J-Y (2011) Characterization of joint roughness in granite by applying the scan circle technique to

- images from a borehole televiewer. *Rock Mech Rock Eng* 44:497–504. <https://doi.org/10.1007/s00603-011-0134-9>
- Bahaaddini M, Hagan P, Mitra R, Hebblewhite B (2014) Scale effect on the shear behaviour of rock joints based on a numerical study. *Eng Geol* 181:212–223. <https://doi.org/10.1016/j.enggeo.2014.07.018>
- Ban L, Du W, Jin T, Qi C, Li X (2021) A roughness parameter considering joint material properties and peak shear strength model for rock joints. *Int J Min Sci Technol* 31:413–420. <https://doi.org/10.1016/j.ijmst.2021.03.007>
- Bandis S, Lumsden A, Barton N (1981) Experimental studies of scale effects on the shear behaviour of rock joints. *Int J Rock Mech Mining Sci Geomech Abstracts* 18:1–21. [https://doi.org/10.1016/0148-9062\(81\)90262-X](https://doi.org/10.1016/0148-9062(81)90262-X)
- Barton N (1978) Suggested methods for the quantitative description of discontinuities in rock masses. *ISRM Int J Rock Mech Mining Sci Geomech Abstracts* 15:319–368
- Barton, N. 1981. Shear strength investigations for surface mining. In; 3rd International Conference on stability surface mining, Vancouver
- Barton, N. 1990. Scale effects or sampling bias. *Scale Effects in Rock Mechanics*, 31–55.
- Chen Y, Lin H, Ding X, Xie S (2021) Scale effect of shear mechanical properties of non-penetrating horizontal rock-like joints. *Environ Earth Sci* 80:1–10. <https://doi.org/10.1007/s12665-021-09485-x>
- Diaz M, Kim KY, Yeom S, Zhuang L, Park S, Min K-B (2017) Surface roughness characterization of open and closed rock joints in deep cores using X-ray computed tomography. *Int J Rock Mech Min Sci* 98:10–19. <https://doi.org/10.1016/j.ijrmms.2017.07.001>
- Du S (1994) Research on mechanical effect of rock joint. *J Grad School China Univ Geosci* 8:198–208
- Du S (1998) Research on complexity of surface undulating shapes of rock joints. *J China Univ Geosci* 9:86–89
- Du S (1999) Engineering behavior of discontinuities in rock mass. Seismological Press, Beijing
- Fardin N (2007) Influence of structural non-stationarity of surface roughness on morphological characterization and mechanical deformation of rock joints. *Rock Mech Rock Eng* 41:267–297. <https://doi.org/10.1007/s00603-007-0144-9>
- Fardin N, Stephansson O, Jing L (2001) The scale dependence of rock joint surface roughness. *Int J Rock Mech Min Sci* 38:659–669. [https://doi.org/10.1016/S1365-1609\(01\)00028-4](https://doi.org/10.1016/S1365-1609(01)00028-4)
- Fardin N, Feng Q, Stephansson O (2004) Application of a new in situ 3D laser scanner to study the scale effect on the rock joint surface roughness. *Int J Rock Mech Min Sci* 41:329–335. [https://doi.org/10.1016/S1365-1609\(03\)00111-4](https://doi.org/10.1016/S1365-1609(03)00111-4)
- Grasselli G (2006) Manuel rocha medal recipient: shear strength of rock joints based on quantified surface description. *Rock Mech Rock Eng* 39:295–314. <https://doi.org/10.1007/s00603-006-0100-0>
- Grasselli G, Wirth J, Egger P (2002) Quantitative three-dimensional description of a rough surface and parameter evolution with shearing. *Int J Rock Mech Min Sci* 39:789–800. [https://doi.org/10.1016/S1365-1609\(02\)00070-9](https://doi.org/10.1016/S1365-1609(02)00070-9)
- Grasselli G (2001) Shear strength of rock joints based on quantified surface description, Ph.D. thesis. EPF Lausanne, Lausanne
- Hencher SR, Richards LR (2014) Assessing the shear strength of rock discontinuities at laboratory and field scales. *Rock Mech Rock Eng* 48:883–905. <https://doi.org/10.1007/s00603-014-0633-6>
- Huang L, Tang H, Wang L, Juang C (2019) Minimum scanline-to-fracture angle and sample size required to produce a highly accurate estimate of the 3-D fracture orientation distribution. *Rock Mech Rock Eng* 52:803–825. <https://doi.org/10.1007/s00603-018-1621-z>
- Kulatilake P, Um J (1999) Requirements for accurate quantification of self-affine roughness using the roughness–length method. *Int J Rock Mech Min Sci* 36:5–18
- Lê HK, Huang W, Liao M, Weng M (2018) Spatial characteristics of rock joint profile roughness and mechanical behavior of a randomly generated rock joint. *Eng Geol*. <https://doi.org/10.1016/j.enggeo.2018.06.017>
- Li Y-R, Zhang Y-B (2015) Quantitative estimation of joint roughness coefficient using statistical parameters. *Int J Rock Mech Min Sci* 77:27–35. <https://doi.org/10.1016/j.ijrmms.2015.03.016>
- Liu X, Zhu W, Yu QL, Chen S, Li R (2017) Estimation of the joint roughness coefficient of rock joints by consideration of two-order asperity and its application in double-joint shear tests. *Eng Geol* 220:243–255. <https://doi.org/10.1016/j.enggeo.2017.02.012>
- Lopez P, Riss J, Archambault G (2003) An experimental method to link morphological properties of rock fracture surfaces to their mechanical properties. *Int J Rock Mech Min Sci* 40:947–954. [https://doi.org/10.1016/S1365-1609\(03\)00052-2](https://doi.org/10.1016/S1365-1609(03)00052-2)
- Maerz N, Franklin J, Bennett C (1990) Joint roughness measurement using shadow profilometry. *Int J Rock Mech Mining Sci Geomech Abstr* 27:329–343
- Morelli GL (2014) On joint roughness: measurements and use in rock mass characterization. *Geotech Geol Eng* 32:345–362
- Murthy MN (1967) Sampling theory and methods. CRC Press
- Palmström A (1995) RMI—a rock mass characterization system for rock engineering purposes. University of Oslo, PhD
- Spiegel MR, Stephens LJ (2017) Schaum's outline of statistics. McGraw Hill Professional
- Tang Z, Huang R, Liu Q, Wong LNY (2015) Effect of contact state on the shear behavior of artificial rock joint. *Bull Eng Geol Env* 75:761–769. <https://doi.org/10.1007/s10064-015-0776-z>
- Tang H, Huang L, Juang CH, Zhang J (2017) Optimizing the Terzaghi estimator of the 3D distribution of rock fracture orientations. *Rock Mech Rock Eng* 50:2085–2099
- Tanyas H, Ulusay R (2013) Assessment of structurally-controlled slope failure mechanisms and remedial design considerations at a field-spar open pit mine, Western Turkey. *Eng Geol* 155:54–68
- Tatone BSA, Grasselli G (2010) A new 2D discontinuity roughness parameter and its correlation with JRC. *Int J Rock Mech Min Sci* 47:1391–1400. <https://doi.org/10.1016/j.ijrmms.2010.06.006>
- Tatone BSA, Grasselli G (2012) An investigation of discontinuity roughness scale dependency using high-resolution surface measurements. *Rock Mech Rock Eng* 46:657–681. <https://doi.org/10.1007/s00603-012-0294-2>
- Tatone B, Grasselli G (2013) An investigation of discontinuity roughness scale dependency using high-resolution surface measurements. *Rock Mech Rock Eng* 46:657–681. <https://doi.org/10.1007/s00603-012-0294-2>
- Tse R, Cruden D (1979) Estimating joint roughness coefficients. *Int J Rock Mech Mining Sci Geomech Abstr* 16:303–307
- Ulusay R, Hudson JA (2006) The complete ISRM suggested methods for rock characterization, testing and monitoring: 1974–2006. International Society for Rock Mechanics Commission on Testing Methods
- Vogler D, Walsh SDC, Bayer P, Amann F (2017) Comparison of surface properties in natural and artificially generated fractures in a crystalline rock. *Rock Mech Rock Eng* 50:2891–2909. <https://doi.org/10.1007/s00603-017-1281-4>
- Wu Q, Jiang Y, Tang H, Luo H, Wang X, Kang J, Zhang S, Yi X, Fan L (2020) Experimental and numerical studies on the evolution of shear behaviour and damage of natural discontinuities at the interface between different rock types. *Rock Mech Rock Eng* 53:3721–3744. <https://doi.org/10.1007/s00603-020-02129-9>
- Xia C, Tang Z, Xiao W, Song Y (2014) New peak shear strength criterion of rock joints based on quantified surface description.

- Rock Mech Rock Eng 47:387–400. <https://doi.org/10.1007/s00603-013-0395-6>
- Yang S, Huang Y, Tian W, Yin P, Jing H (2019a) Effect of high temperature on deformation failure behavior of granite specimen containing a single fissure under uniaxial compression. *Rock Mech Rock Eng*. <https://doi.org/10.1007/s00603-018-1725-5>
- Yang S, Yin P, Zhang Y, Chen M, Zhou X, Jing H, Zhang Q (2019b) Failure behavior and crack evolution mechanism of a non-persistent jointed rock mass containing a circular hole. *Int J Rock Mech Mining Sci* 114:101–121. <https://doi.org/10.1016/j.ijrmms.2018.12.017>
- Ye J (2014) Vector similarity measures of simplified neutrosophic sets and their application in multicriteria decision making. *Int J Fuzzy Syst* 16:204–211
- Ye J, Yong R, Liang Q, Huang M, Du S (2016) Neutrosophic functions of the joint roughness coefficient and the shear strength: a case study from the pyroclastic rock mass in Shaoxing City, China. *Math Probl Eng*. <https://doi.org/10.1155/2016/4825709>
- Yong R, Fu X, Huang M, Liang Q, Du S (2018a) A rapid field measurement method for the determination of Joint Roughness Coefficient of large rock joint surfaces. *KSCE J Civ Eng* 22:101–109. <https://doi.org/10.1007/s12205-017-0654-2>
- Yong R, Qin J, Huang M, Du S, Liu J, Hu G (2018b) An innovative sampling method for determining the scale effect of rock joints. *Rock Mech Rock Eng*. <https://doi.org/10.1007/s00603-018-1675-y>
- Yong R, Ye J, Li B, Du S (2018c) Determining the maximum sampling interval in rock joint roughness measurements using Fourier series. *Int J Rock Mech Min Sci* 101:78–88. <https://doi.org/10.1016/j.ijrmms.2017.11.008>
- Yong R, Ye J, Liang Q, Huang M, Du S (2018d) Estimation of the joint roughness coefficient (JRC) of rock joints by vector similarity measures. *Bull Eng Geol Env* 77:735–749. <https://doi.org/10.1007/s10064-016-0947-6>
- Zhang G, Karakus M, Tang H, Ge Y, Zhang L (2014) A new method estimating the 2D Joint Roughness Coefficient for discontinuity surfaces in rock masses. *Int J Rock Mech Min Sci* 72:191–198. <https://doi.org/10.1016/j.ijrmms.2014.09.009>
- Zhang X, Jiang Q, Chen N, Wei W, Feng X (2016) Laboratory investigation on shear behavior of rock joints and a new peak shear strength criterion. *Rock Mech Rock Eng* 49:3495–3512. <https://doi.org/10.1007/s00603-016-1012-2>
- Zhang G, Karakus M, Tang H, Ge Y, Jiang Q (2017) Estimation of joint roughness coefficient from three-dimensional discontinuity surface. *Rock Mech Rock Eng* 50:2535–2546. <https://doi.org/10.1007/s00603-017-1264-5>
- Zhao L, Zhang S, Huang D, Zuo S, Li D (2018) Quantitative characterization of joint roughness based on semivariogram parameters. *Int J Rock Mech Min Sci* 109:1–8. <https://doi.org/10.1016/j.ijrmms.2018.06.008>
- Zheng B, Qi S (2016) A new index to describe joint roughness coefficient (JRC) under cyclic shear. *Eng Geol* 212:72–85. <https://doi.org/10.1016/j.enggeo.2016.07.017>

Publisher's Note Springer Nature remains neutral with regard to jurisdictional claims in published maps and institutional affiliations.